Technical Report Documentation Page

1. Report No.	2. Government Accession No.	3. Recipient's Catalog No.
FHWA/TX-92/1233-1		

4. Title and Subtitle	5. Report Date
IMPLEMENTATION OF THE TEXAS GROUND PENETRATING RADAR SYSTEM	November 1992 Revised: April 1994
	6. Performing Organization Code
7. Author(s)	8. Performing Organization Report No.
Tom Scullion, Chun-Lok Lau, and Yiqing Chen	Research Report 1233-1
9. Performing Organization Name and Address	10. Work Unit No. (TRAIS)
Texas Transportation Institute The Texas A&M University System College Station, Texas 77843-3135	11. Contract or Grant No. Study No. 0-1233
12. Sponsoring Agency Name and Address	13. Type of Report and Period Covered
Texas Department of Transportation Research and Technology Transfer Office P. O. Box 5080 Austin, Texas 78763-5080	Interim: September 1989-September 1992
	14. Sponsoring Agency Code

15. Supplementary Notes

Research performed in cooperation with the Texas Department of Transportation and the U.S. Department of Transportation, Federal Highway Administration.
Research Study Title: New Technologies for Pavement Evaluation

16. Abstract

Ground Penetrating Radar is a nondestructive testing tool for evaluating pavements. The system described in this report uses an air launched antenna which is suspended between 10 and 14 inches above the pavement and has been shown capable of operating adequately at close to highway speed (± 40 mph). This report describes the system developed and implemented for TxDOT. The system includes a Penetradar PS-24 Ground Penetrating Radar system, a TTI developed data acquisition and signal processing system, a data acquisition vehicle housing a Distance Measuring Instrument and synchronized video recording system. The hardware, software and data processing procedures will be described together with several case studies in which GPR has been used to evaluate pavement rehabilitation jobs in Texas. These applications include layer thickness determination, void detection, base course evaluation and locating areas of asphalt stripping.

17. Key Words	18. Distribution Statement
Ground Penetrating Radar, GPR, Pavements, Data Acquisition, Thickness, Voids	No Restrictions. This document is available to the public through NTIS: National Technical Information Service 5285 Port Royal Road Springfield, Virginia 22161

19. Security Classif.(of this report)	20. Security Classif.(of this page)	21. No. of Pages	22. Price
Unclassified	Unclassified	102	

Form DOT F 1700.7 (8-72) Reproduction of completed page authorized

IMPLEMENTATION OF THE TEXAS GROUND PENETRATING RADAR SYSTEM

by

Tom Scullion
Associate Research Engineer
Texas Transportation Institute

Chun-Lok Lau
Engineer Research Associate
Texas Transportation Institute

and

Yiqing Chen
Graduate Assistant Research
Texas Transportation Institute

Research Report 1233-1
Research Study Number 0-1233
Research Study Title: New Technologies for Pavement Evaluation

Sponsored by the
Texas Department of Transportation
In Cooperation with
U.S. Department of Transportation
Federal Highway Administration

November 1992
Revised: April 1994

TEXAS TRANSPORTATION INSTITUTE
Texas A&M University System
College Station 77843-3135

METRIC (SI*) CONVERSION FACTORS

APPROXIMATE CONVERSIONS TO SI UNITS

Symbol	When You Know	Multiply By	To Find	Symbol
LENGTH				
in	inches	2.54	centimetres	cm
ft	feet	0.3048	metres	m
yd	yards	0.914	metres	m
mi	miles	1.61	kilometres	km
AREA				
in^2	square inches	645.2	centimetres squared	cm^2
ft^2	square feet	0.0929	metres squared	m^2
yd^2	square yards	0.836	metres squared	m^2
mi^2	square miles	2.59	kilometres squared	km^2
ac	acres	0.395	hectares	ha
MASS (weight)				
oz	ounces	28.35	grams	g
lb	pounds	0.454	kilograms	kg
T	short tons (2000 lb)	0.907	megagrams	Mg
VOLUME				
fl oz	fluid ounces	29.57	millilitres	mL
gal	gallons	3.785	litres	L
ft^3	cubic feet	0.0328	metres cubed	m^3
yd^3	cubic yards	0.0765	metres cubed	m^3

NOTE: Volumes greater than 1000 L shall be shown in m^3.

TEMPERATURE (exact)

°F	Fahrenheit temperature	5/9 (after subtracting 32)	Celsius temperature	°C

APPROXIMATE CONVERSIONS TO SI UNITS

Symbol	When You Know	Multiply By	To Find	Symbol
LENGTH				
mm	millimetres	0.039	inches	in
m	metres	3.28	feet	ft
m	metres	1.09	yards	yd
km	kilometres	0.621	miles	mi
AREA				
mm^2	millimetres squared	0.0016	square inches	in^2
m^2	metres squared	10.764	square feet	ft^2
km^2	kilometres squared	0.39	square miles	mi^2
ha	hectores (10 000 m^2)	2.53	acres	ac
MASS (weight)				
g	grams	0.0353	ounces	oz
kg	kilograms	2.205	pounds	lb
Mg	megagrams (1 000 kg)	1.103	short tons	T
VOLUME				
mL	millilitres	0.034	fluid ounces	fl oz
L	litres	0.264	gallons	gal
m^3	metres cubed	35.315	cubic feet	ft^3
m^3	metres cubed	1.308	cubic yards	yd^3

TEMPERATURE (exact)

°C	Celsius temperature	9/5 (then add 32)	Fahrenheit temperature	°F

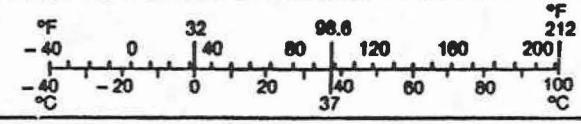

These factors conform to the requirement of FHWA Order 5190.1A.

* SI is the symbol for the International System of Measurements

IMPLEMENTATION STATEMENT

This study has demonstrated that GPR has the ability to assist TxDOT in pavement evaluation. GPR's ability to measure asphalt layer thickness has been documented in this and in complementary TTI reports 930-5F and 1923-1F. This study also validates that GPR can be used to detect moisture related problems beneath concrete slabs (voids) and in asphalt layers (stripping).

It is concluded that the system developed in this project can be implemented within the TxDOT system to either complement existing NDT testing (such as FWD) or to provide additional capabilities. At the network level it can be used to establish a layer thickness data base and identify homogeneous sections for PMS applications. At the project level it can work in coordination with the FWD when layer thicknesses are unknown. Perhaps the most potential is in the area of project level evaluation prior to rehabilitation design. GPR can be used at high speed to locate potential problem areas within the pavement layers before any coring is performed.

DISCLAIMER

This report is not intended to constitute a standard, specification or regulation and does not necessarily represent the views or policy of the FHWA or Texas Department of Transportation. Additionally, this report is not intended for construction, bidding, or permit purposes. The engineer in charge of the project was Tom Scullion P.E. # 62683.

ACKNOWLEDGMENTS

The authors would like to acknowledge the Texas State Department of Transportation, particularly Mssrs. Rob Harris, P.E. and Bob Briggs P.E., for their interest and support of this work. John Ragsdale of TTI, assembled the test vehicle and supervised the field data collection. Dr. Ken Maser of Infrasense was a consultant to TTI on the two companion studies. Ken contributed in many areas, including developing the field data collection protocol and providing constructive guidance in the development of the data processing software.

TABLE OF CONTENTS

TABLE OF CONTENTS (CONTINUED)

LIST OF FIGURES

LIST OF FIGURES (Continued)

LIST OF FIGURES (Continued)

LIST OF TABLES

SUMMARY

Ground Penetrating Radar is a nondestructive testing tool for evaluating pavements. The system described in this report uses an air launched antenna which is suspended between 10 and 14 inches above the pavement and has been shown capable of operating adequately at close to highway speed (± 40 mph). This report describes the system developed and implemented for the TxDOT. The system includes a Penetradar PS-24 Ground Penetrating Radar system, a TTI developed data acquisition and signal processing system, a data acquisition vehicle housing a Distance Measuring Instrument and synchronized video recording system. The hardware, software and data processing procedures will be described together with several case studies in which GPR has been used to evaluate pavement rehabilitation jobs in Texas. These applications include layer thickness determination, void detection, base course evaluation and locating areas of asphalt stripping.

1. INTRODUCTION

Principles of Ground Penetrating Radar

Ground Penetrating Radar operates by transmitting short pulses of electromagnetic energy into the pavement. These pulses as shown in Figure 1 are reflected back to the antenna with the amplitude and arrival time that is related to the electrical properties of the pavement layers. The reflected energy is collected and displayed as a waveform; a typical example showing amplitudes and arrival times of reflections is shown in Figure 2. This is a flexible pavement consisting of seven inches of hot mix over a six inch granular base over a clay subgrade. The large peak (A) at 6 nanoseconds is the energy reflected from the surface; the peaks (B) and (C) represent reflections from the top of the base and subgrade respectively. The time interval between peaks (A) and (B) is the travel time for the radar wave to travel from the surface to the top of the base and back (twice the asphalt thickness). The speed with which the electromagnetic radar wave travels in a particular layer is related to the dielectric constant of that layer. It is also the dielectric which determines what percentage of the energy is transmitted and reflected at each layer interface.

In pavements the parameter that most influences the dielectric properties of materials is the moisture content. Table 1 shows a table of dielectrics for typical pavement materials. As can be seen from this table the addition of moisture to any of these materials will have a significant influence on the dielectric properties of that layer. For example, a dry limestone base course with 4% by weight of moisture will have a dielectric of around 6; if the moisture content increases to 10%, then the dielectric of the layer would increase to around 11. The impact of a wet base on the trace shown in Figure 2 would be to increase the amplitude of peak B and to increase the travel time between peaks B and C.

The fact that GPR is sensitive only to changes in dielectric, which mostly equates to changes in layer moisture content, is of major significance. Without these differences in electrical properties, no energy will be reflected at interfaces. Several cases exist in pavements where the layers are so similar electrically that no significant reflections will be detected. Cases like this are common, such as granular base over sand subgrade, or concrete over cement stabilized bases. In these cases the

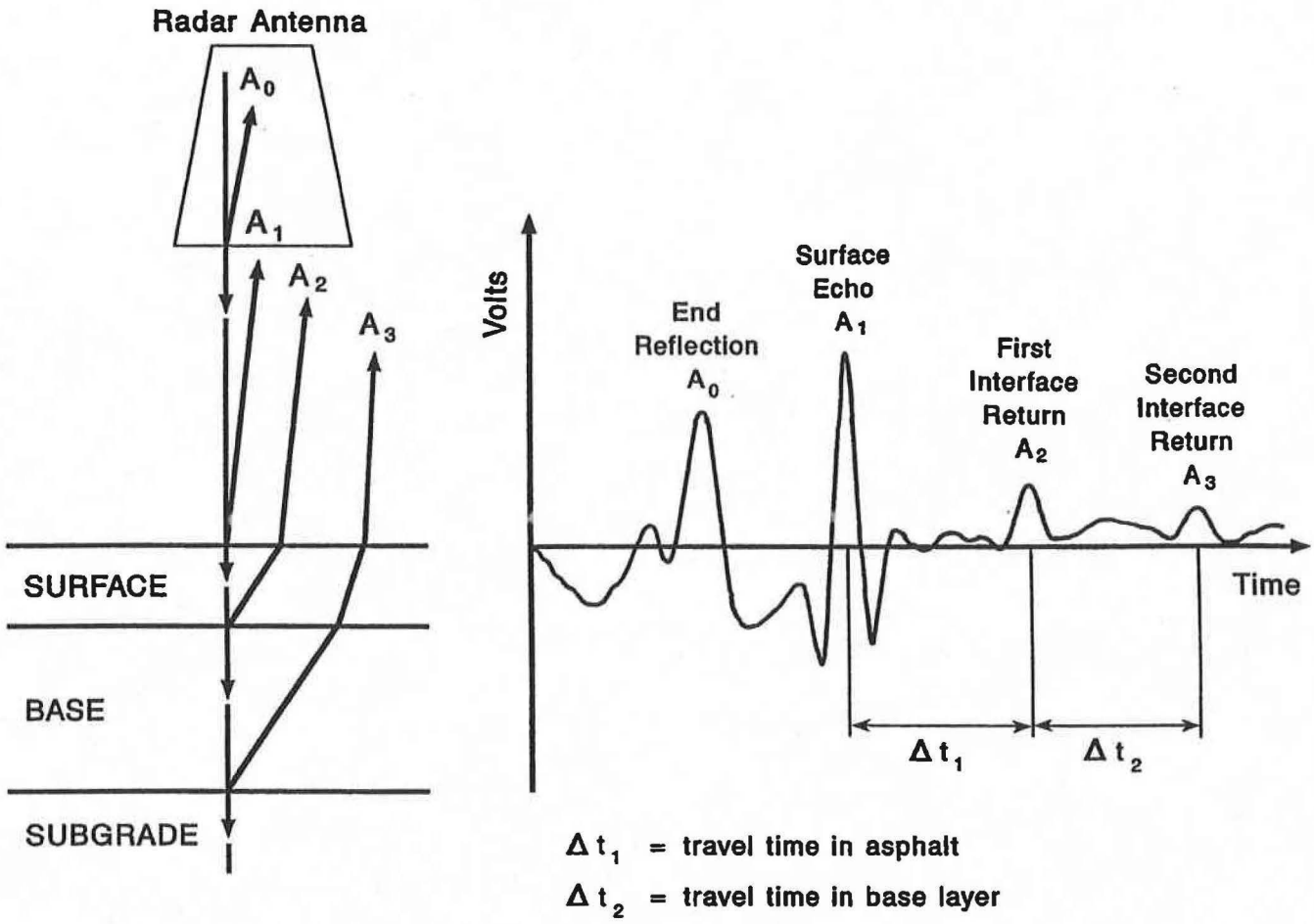

Figure 1. Principles of Ground Penetrating Radar. The Incident Wave is Reflected at each Layer Interface and Plotted as Return Voltage Against Time of Arrival in Nanoseconds.

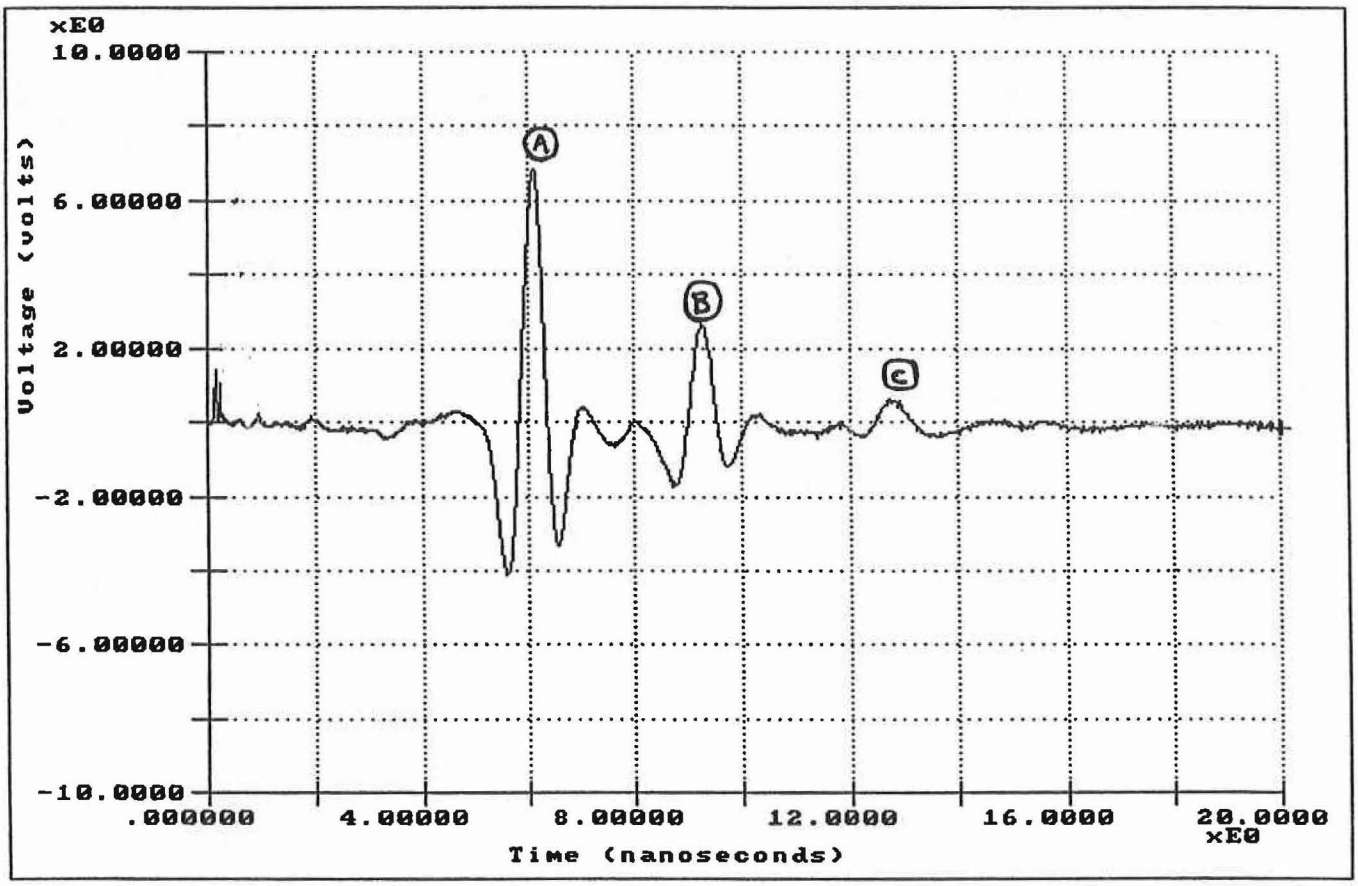

Figure 2. Typical GPR Waveform. Peaks A, B and C are Reflections from the Surface, Top of the Base and Top of the Subgrade Respectively.

Table 1. Typical Dielectrics for Highway Materials.

Material	Dielectric Constant
Air	1
Water	81
Asphalt	3 - 6
Concrete	6 - 11
Limestone	4 - 8
Clays	5 - 40
Dry Sand	3 - 5
Saturated Sand	20 - 30

electrical difference between layers may not be sufficient to permit layer thickness estimates.

The majority of GPR signal processing in the highway field to date has relied upon "expert" interpretation of stacked, sometimes color coded, multiple radar traces. The expert locates anomalies such as voids by identifying certain colored areas on the display screen. However, several DOT's, although recognizing potential in GPR, have been disappointed with the expert interpretation. The fundamental approach taken in this study has been somewhat different. Efforts have been made to develop signal processing techniques to interpret individual GPR waveforms. Without the ability to interpret a single trace it may be difficult to process multiple traces. To use automated signal processing techniques it is necessary to utilize a GPR system with clean, repeatable transmitted pulses of GPR energy. As part of this study, it was found necessary to develop specifications of radar performance. These will be described in Section 2.

The software developed as part of this study is described in Section 3 of this report. This software automatically measures the amplitudes and time delays of each radar trace received and applies the signal processing described below. Figure 2 shows a single trace from a section of highway. The user can specify the frequency at which traces are to be collected. In some instances, such as void detection, one trace per foot of pavement may be required. In others, such as layer thickness inventorying, one measurement (one trace) per 100 feet may be adequate. In either case a typical radar survey consists of collections and processing multiple traces similar to the one shown in Figure 2.

The principles of GPR applied to highways have been given elsewhere (Maser and Scullion 1991). By automatically monitoring the amplitudes and time delays between peaks, it is possible to calculate layer dielectrics, layer thicknesses and to estimate the moisture content of granular base material. These equations are summarized below [see Maser and Scullion 1991 for derivations].

$$\epsilon_a = \left[\frac{1 + A_o/A_m}{1 - A_o/A_m}\right]^2 \qquad (1)$$

where

ϵ_a = the dielectric of the asphalt or concrete surfacing layer

A_o = the amplitude of reflection from the surface in volts (peak A in Figure 2)

A_m = the amplitude of reflection from a large metal plate in volts (this represents the 100% reflection case)

$$h_1 = \frac{c \times \Delta t_1}{\sqrt{\epsilon_a}} \tag{2}$$

where

h_1 = the thickness of top layer

c = a constant obtained from the time calibration procedure described in section 3 of this report

Δt_1 = the time delay between peaks A and B of Figure 2

$$\sqrt{\epsilon_b} = \sqrt{\epsilon_a}\left[\frac{1 - \left[\frac{A_o}{A_m}\right]^2 + \left[\frac{A_1}{A_m}\right]}{1 - \left[\frac{A_o}{A_m}\right]^2 - \left[\frac{A_1}{A_m}\right]}\right] \tag{3}$$

where

ϵ_b = the dielectric of the base layer

A_1 = the amplitude of reflection from the top of the base layer in volts (peak B in Figure 2)

$$M = \frac{\sqrt{\epsilon_b} - 1 - \gamma(\sqrt{\epsilon_s} - 1)}{\sqrt{\epsilon_b} - 1 - \gamma(\sqrt{\epsilon_s} - 22.2)} \tag{4}$$

where

M = the moisture content of base (% of total wt.)

ϵ_s = solids dielectric constant (varies from 4 to 8 depending on source material)

γ = dry density γ_d (lbs/ft^3) divided by density of solids γ_s (~165 lbs/ft^3)

Note equation 4 assumes that the density along a highway remains constant. This clearly is not the case and will limit the accuracy of moisture content estimation. However, the moisture content is the major factor which influences measured base dielectric constant ϵ_b. The relative dielectric constants of air, dry granular base and water are approximately 1, 6, and 81 respectively. High base dielectrics are almost certainly attributable to high moisture contents. The accuracy of equation 4 is yet to be determined.

The above equations serve as the basis for analysis of the data collected during this study, as described below. They are based on the assumption that the layer materials are non-conductive and homogenous. This assumption means that the imaginary component of the dielectric constant tends to zero; and therefore the medium does not attenuate the radar signal. Therefore all of the energy is either reflected or transmitted and none is lost in heating free water in the layer. The assumption of a very low imaginary dielectric from laboratory tests at the Texas Transportation Institute appears to be reasonable for asphalt concrete hot mix. However, it does not seem to be the case for either concrete or wet base course material. Because of the higher attenuation, it is thought that the accuracy of layer thickness estimates for both concrete layers and granular base layers may be less than for hot mix layers. The layer thickness estimates for hot mix asphalts was found to be very good (Maser, Scullion and Briggs, 1991). The accuracy on granular base courses was reasonable, but this was also tied to the inability to physically measure the thickness of existing bases given the intrusion of subgrade materials. The accuracy of these equations for measuring concrete thicknesses is the subject of current research efforts.

Outline of Report

In the next section of this report the GPR system and field data collection system will be described together with the set-up tests conducted during each survey. In section 3 a description will be given of the software used to process the collected GPR waveforms. Section 4 will present several case studies from in-service pavements in Texas.

2. DESCRIPTION OF FIELD UNIT

2.1 Hardware

The Texas Transportation Institute GPR system consists of the following components:

a) A Penetradar Model PS-24 (Penetradar, 1991)
b) A trigger conditioning circuit
c) Data acquisition board
d) Computer and software
e) Distance Measuring Instrument
f) Video acquisition system

Each will be described below.

a) Penetradar Model PS-24

The GPR system was supplied by Penetradar Corporation of Niagara Falls, New York. The system transmits a signal approximately one nanosecond (1 x 10^{-9} seconds) duration with an occurrence rate or pulse repetition frequency of 5 million times per second (5MHz). The signal is radiated through a wide band antenna into the pavement. The signal is air launched, with the antenna usually mounted between 10 and 14 inches above the pavement surface. Each transmitted pulse is reflected from the surface and from each significant layer interface. These radar echoes (waveforms) are intercepted by the same antenna and downsampled by the receiver circuitry. The sampling process permits the user to access 50 waveforms per second over a real time 20 nanosecond range sweep.

The antenna and control box, housing the transmitter and receiving circuitry, are shown in Figure 3. These are attached to the front of the data collection vehicle. The power supply box for the system is shown in Figure 4. The transmitted pulse for the system is shown in Figure 5; it is typically 3 to 6 volts peak to peak and approximately one nanosecond in duration. The transmitter signal is passed through a common junction in the receiver module, through the antenna coaxial line feed, through and out of the end of the antenna. At each of these transition points some energy is reflected; this is shown in Figure 6. The actual reflection from the surface is the last large peak, all preceding peaks are internal noise from the system. In a well tuned system, the internal noise is somewhat smaller

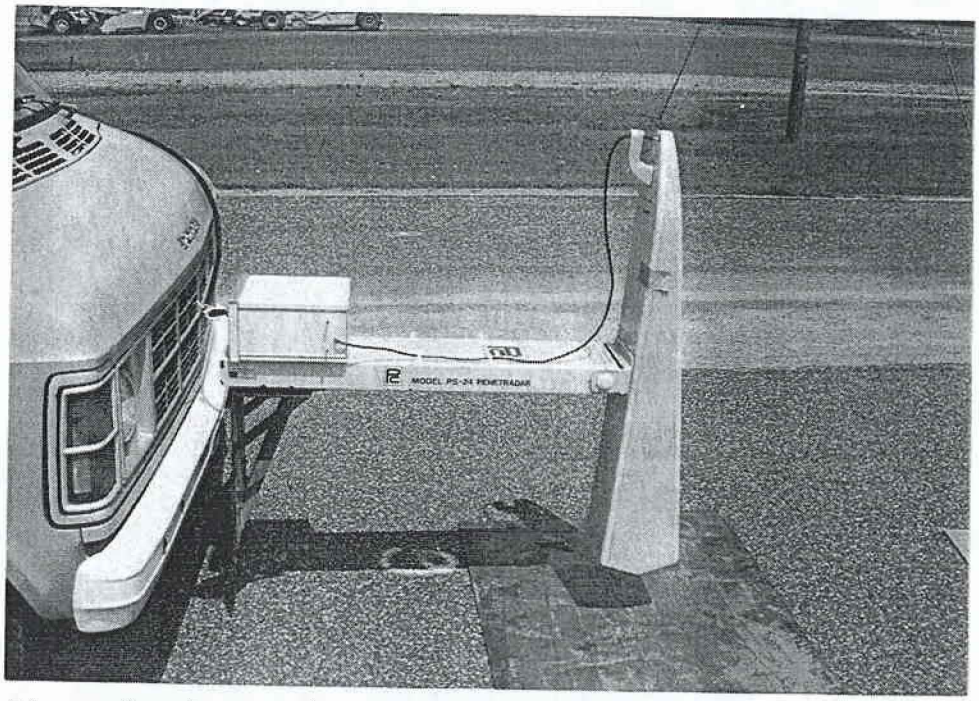

Figure 3. Penetradar Antenna in Test Position.

Figure 4. Power Supply Box Located in Test Vehicle.

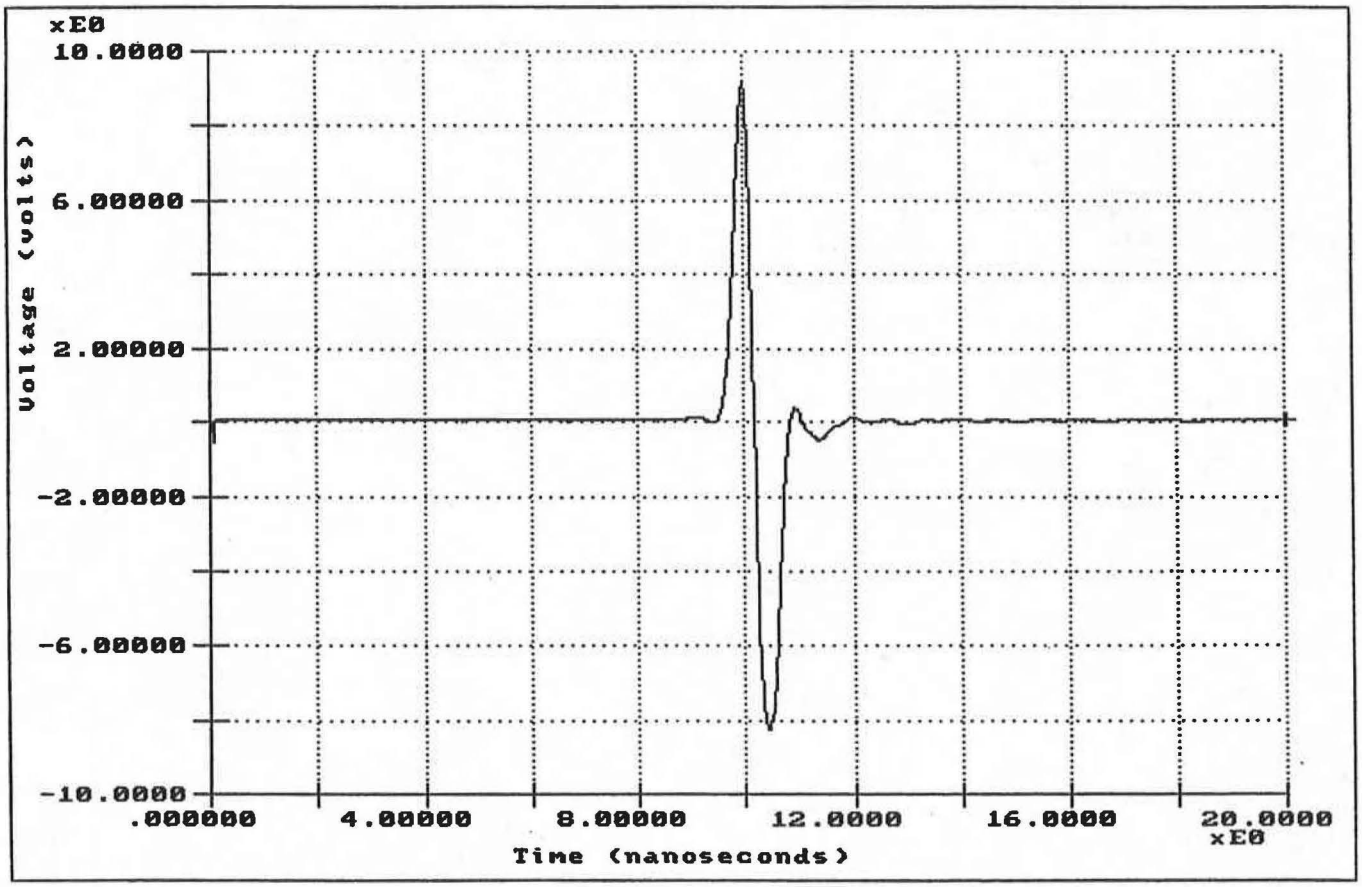

Figure 5. Transmit GPR Pulse (voltage gain = 2.5).

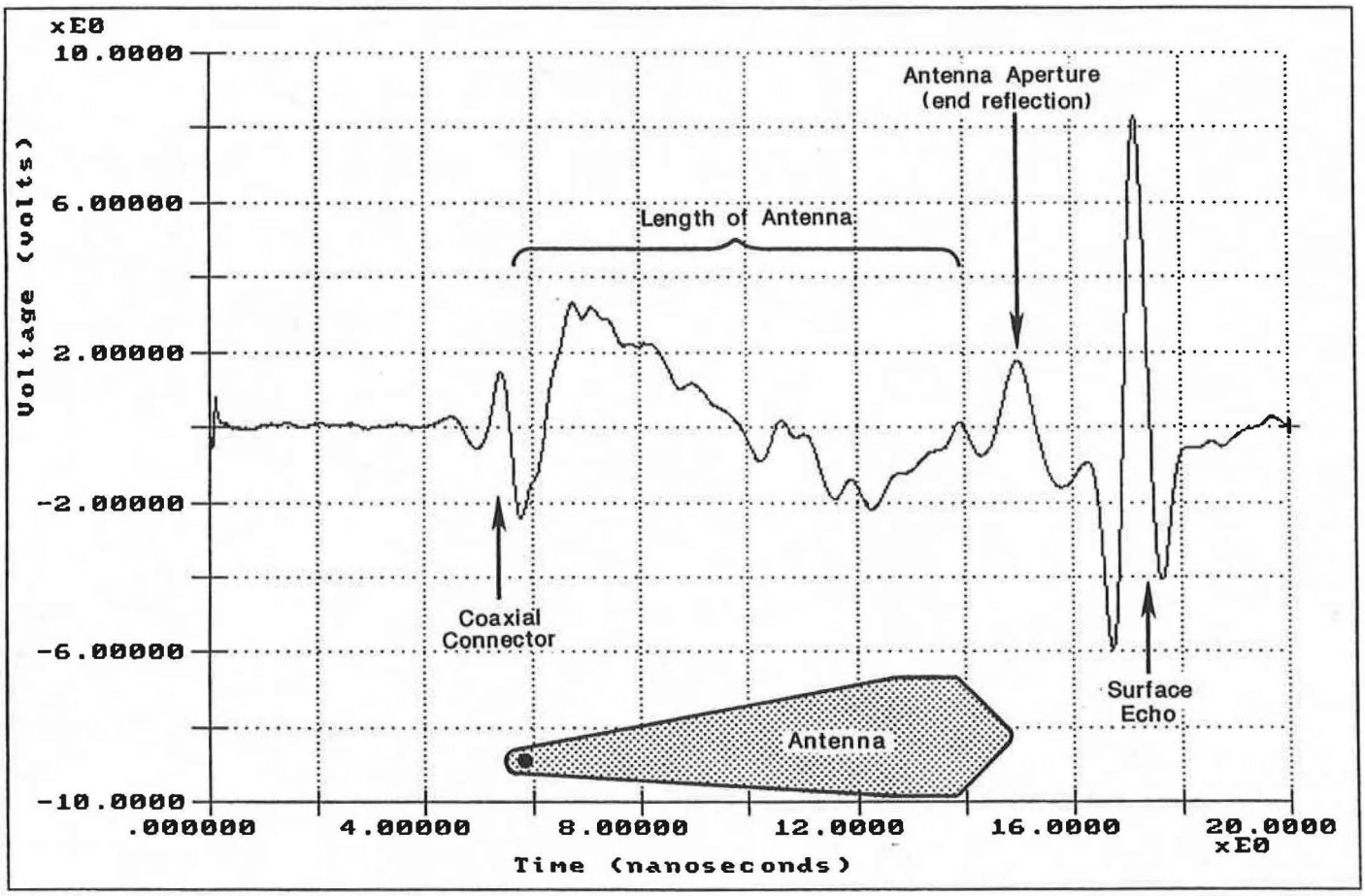

Figure 6. Sources of End Reflection Clutter Preceding Surface Echo.

in amplitude than that from the pavement surface. The information from the pavement layers occurs after the surface reflection. The internal noise preceding the pavement reflections is not a problem with data collection. The PS-24 circuitry permits the user to adjust the 20 nanosecond sweep range, thus the waveform is essentially shifted to the left so that most of the internal clutter is outside the 20 nanosecond window. When collecting data the operator typically adjusts the signal to the left so that the surface reflection occurs between 4 and 6 nanoseconds. Also, as will be described in the next section, a post processing procedure has been developed by which the remaining end reflection can be subtracted from the signal.

b) Triggering Conditioning Circuit

This consists of a single integrated circuit SN74123, a resistor and capacitor. It essentially triggers the data acquisition system. The Penetradar system outputs a square wave when data has been collected. This square wave is transformed into the appropriate trigger signal for the data acquisition board.

c) Data Acquisition Board

The Data Translation product DT2821DI is used to capture and digitize the radar waveforms.

d) Computer and Software

The software developed on this project is described in section 3 of this report. The software is written using the ASYST (ASYST, 1991) data acquisition and analysis environment. To run the system the following computer system is required:

- IBM compatible microcomputer with 386/25MHz microprocessor (or higher)
- 4MB combined conventional, extended and expanded memory
- DOS 5.0 or higher
- A hard disk with 400 MB available storage space and 17 ms or faster IDE time
- VGA graphics adaptor card with 256kb or more memory
- A laser or dot matrix printer.

The collected radar waveforms are displayed on the screen as the unit moves along the highway; a typical waveform collected during data acquisition is shown in Figure 7.

e) Distance Measuring Instrument

During testing GPR waveforms are captured at user defined intervals along the highway, usually ranging from 1 to 10 feet. A Distance Measuring Instrument (DMI) is used to locate each trace. The DMI is a Roadstar 40 system, a product of Nu-Metrics, Inc. The DMI in feet from the start of the project, is included in the data record containing the radar waveform as the last 4 bytes of the record.

f) Video Acquisition System

An integral part of the system is a video log system which collects images of the highway as the GPR data is being collected. The Radar DMI information is also included as a header on the video image. A standard VHS video recorder is used to store the images. Therefore when anomalies are found in the GPR waveforms, it is possible to obtain a video image of that section of pavement. The video camera attachment to the test vehicle is shown in Figure 8.

2.2 Field Test Procedures

This section describes the typical data collection sequence for a GPR survey. Prior to collecting, the following standard set-up procedure is used.

a) System Warm-up

Prior to collecting any waveforms the GPR unit is switched on and allowed to warm-up for a period of 10 minutes. It was found that in the first few minutes of operation there is a steady decrease in the amplitude of reflection from a fixed object. However, after approximately 10 minutes, the reflection amplitude becomes relatively constant.

b) Metal Plate Reflection

The antenna is mounted on the boom shown earlier in Figure 3 and set at the height to be used for data collection. This height is typically fixed at between 10 to 14 inches. A large metal plate (4 ft x 4 ft) is then placed at the surface (this setup is shown in Figure 3) and the 100% reflection case is recorded by the data acquisition system. A typical raw metal plate reflection is shown in Figure 9. As mentioned earlier the

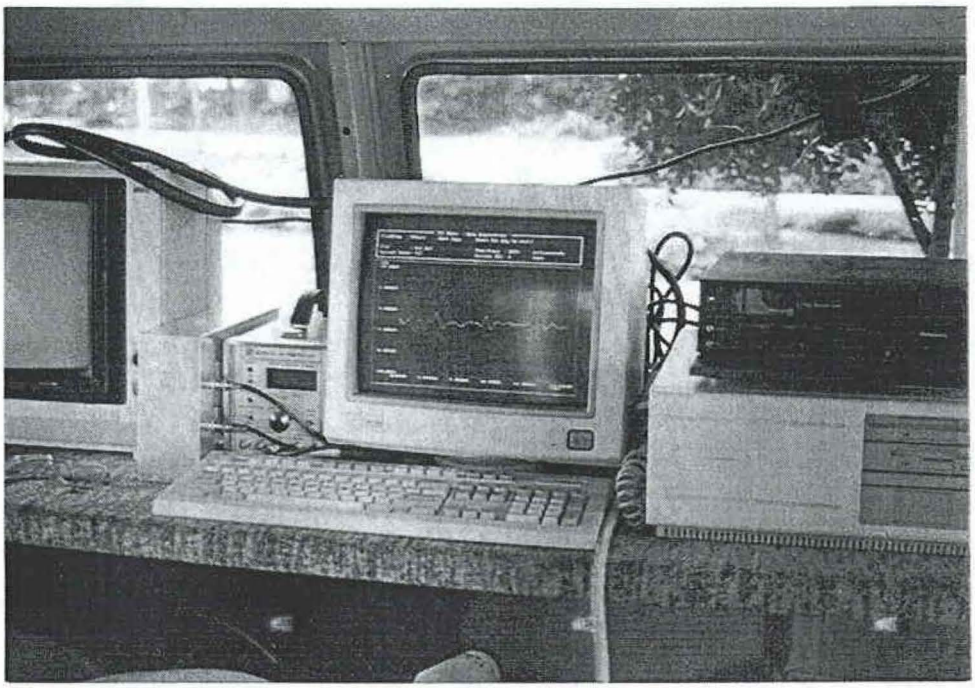

Figure 7. Display Showing GPR Waveforms During Data Acquisition.

Figure 8. Video Acquisition System (DMI Information Added as a Header to the Video Image).

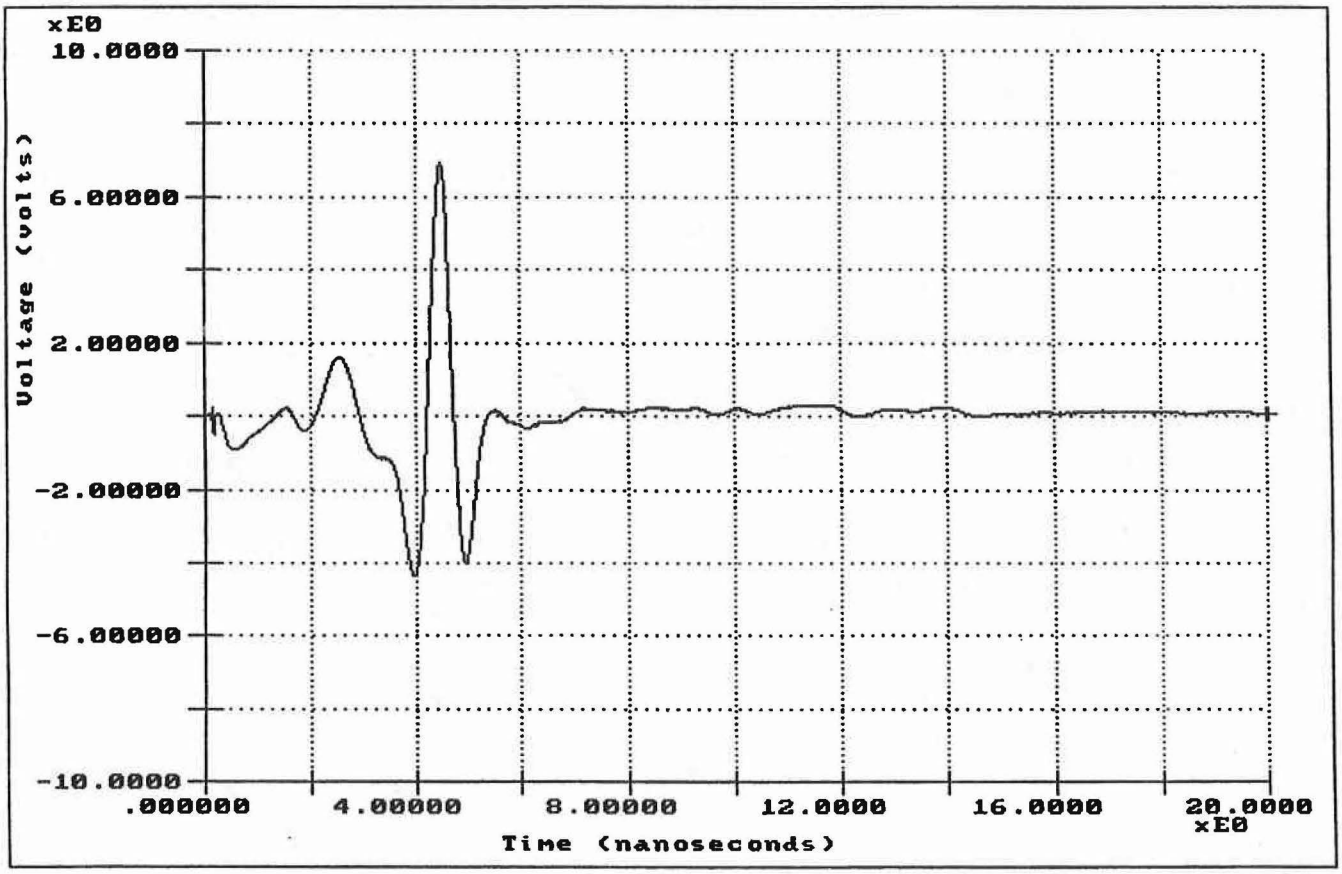

Figure 9. Typical Metal Plate Reflection.

operator has control of the 20 nanosecond recording window. Typically the operator sets the window so that the peak surface reflection occurs at approximately 4 nanoseconds; the window of 15 to 16 nanoseconds after the peak is for reflections from the pavement layers. The end reflection is shown in Figure 9 preceding as the smaller peak before the large metal plate reflection. The end reflection is caused by impedance mismatch at the end of the antenna. One problem is that the tail of the end reflection overlaps into the metal plate reflection. The first step in the signal processing is to align and subtract the end reflection so that the true amplitude of metal plate reflection can be obtained; this technique is demonstrated in section 3 of this report. After the metal plate test, typically the test section is run with radar collected at whatever testing interval is required. Immediately following the collection of the actual data, two additional tests are conducted; these are the end reflection and time calibration test.

c) End Reflection

The antenna is pointed directly up into the air so that no reflections are possible in the 20 nanosecond window. The typical end reflection waveform is shown in Figure 10. The shape and amplitude of this end reflection has been found to be fairly constant with the PENETRADAR system. This end reflection waveform is superimposed on every waveform collected with the system; its removal is discussed in section 3.2.

d) Time Calibration Test

Equation 2 presented earlier is used for layer thickness calculations. The constant c in that equation is computed in this test. The test set-up is shown in Figure 11. A GPR trace is obtained with a metal plate resting

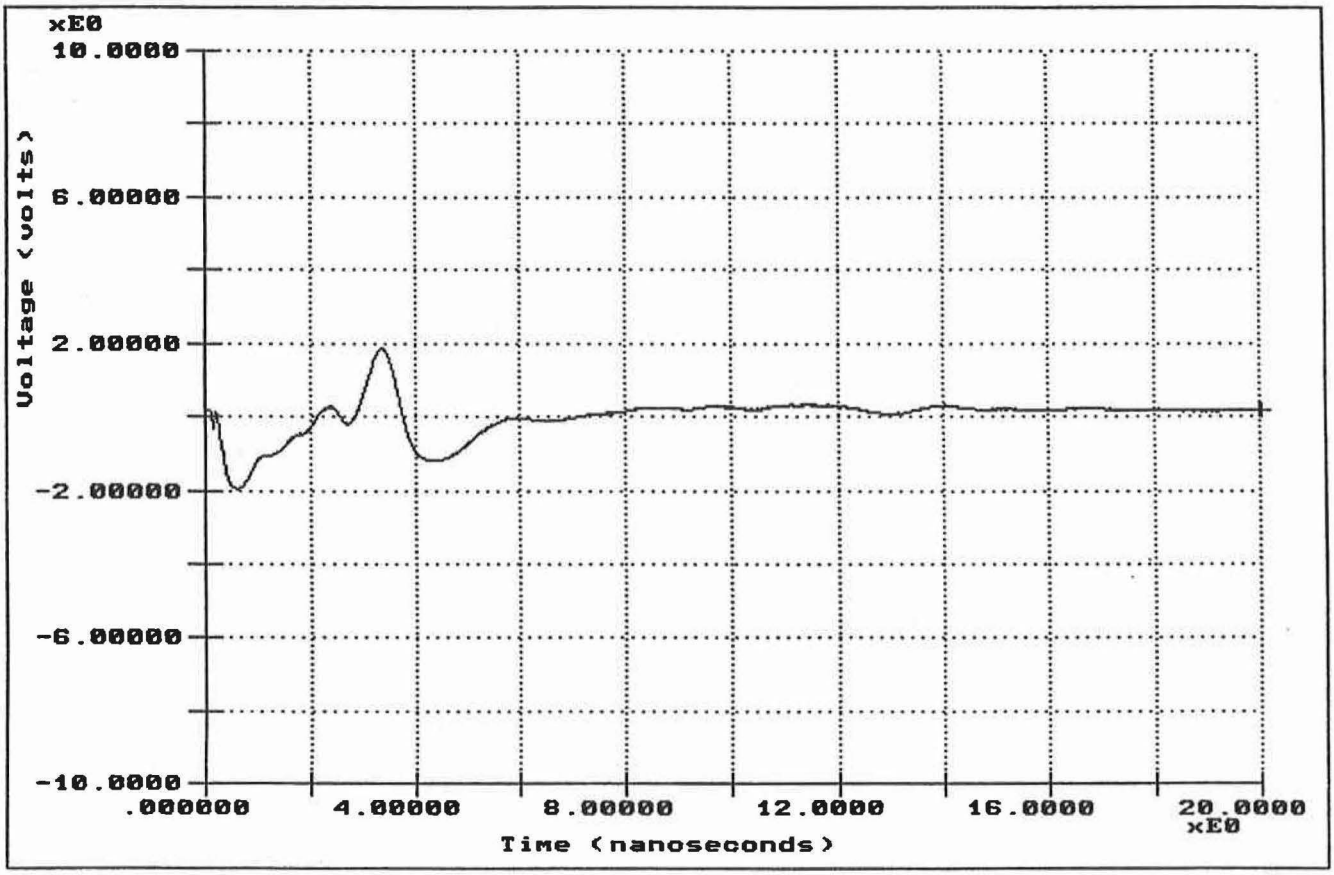

Figure 10. Typical End Reflection. (System Noise which is Superimposed on Each Waveform Collected)

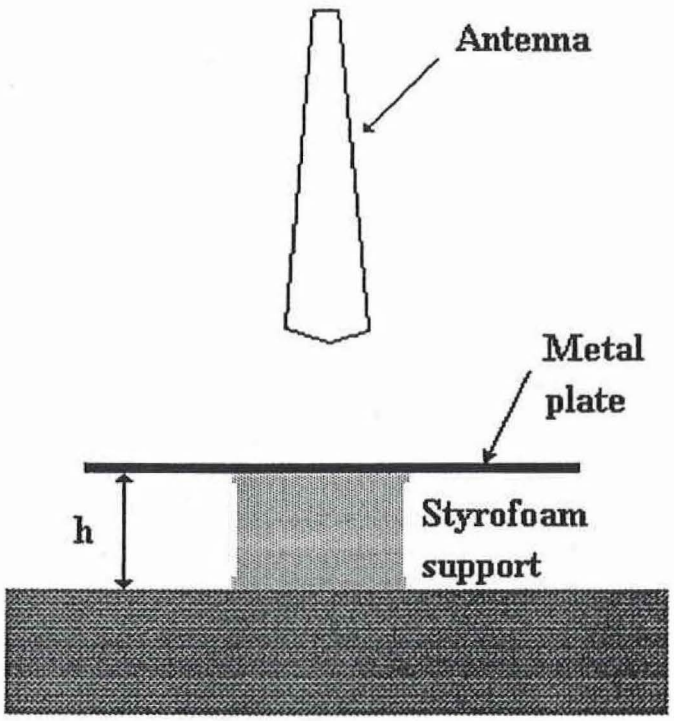

Figure 11. Time Calibration Test Set-up.

on top of a block of fixed height (usually 12 inches). The block is removed and the plate is placed on the ground. A second GPR trace is taken. Using the end reflection peak as a reference, it is possible to calculate the time of travel of twice the thickness of the block. With the relative dielectric of air being 1, the constant c can be calculated from Equation 2.

The constant c should be the speed of light, with the travel time measured in nanoseconds and h in inches. The value of c should be 5.9 ins/nanosecond. However, calibration values of the order of 5.1 to 5.2 are frequently found. This is presumably caused by errors in the systems time base corrector. As described later, the calculated time calibration factor (c) is entered into the data processing system.

2.3 Laboratory Test Set-up

a) Height Calibration

One problem with high speed data acquisition with the antenna suspended in front of the vehicle is that, no matter what the mounting system, the antenna will bounce significantly as it traverses moderately rough highways. On a concrete pavement, movements of ± 1.5 inches have been measured. The method of calculating bounce is to determine the time delay between the system end reflection peak and the surface reflection shown in Figure 9. This time is related to the travel time in air for a journey from the end of the antenna to the surface and back.

It must be remembered that when the layer thickness calculation is being made the system compares the pavement response with the comparable response from a metal plate at the same height to calculate the layer dielectric using equation 1. The pavement response is measured as the vehicle moves down the highway. However, only a single height metal plate reflection is input. To compensate for the "bounce", the system has a height calibration function built into it. This was developed by simply measuring voltage reflection amplitudes from a large metal plate at various heights as shown in Figure 12. The shape of this curve is used to adjust the input metal plate amplitude. When processing radar traces, the time delay between the end reflection and the surface echo (D_t in Figure 12) is computed for each trace, and the corresponding amplitude adjustment factor is calculated. This factor is used to adjust the input metal plate amplitude in the layer thickness calculation. Assuming the relationship

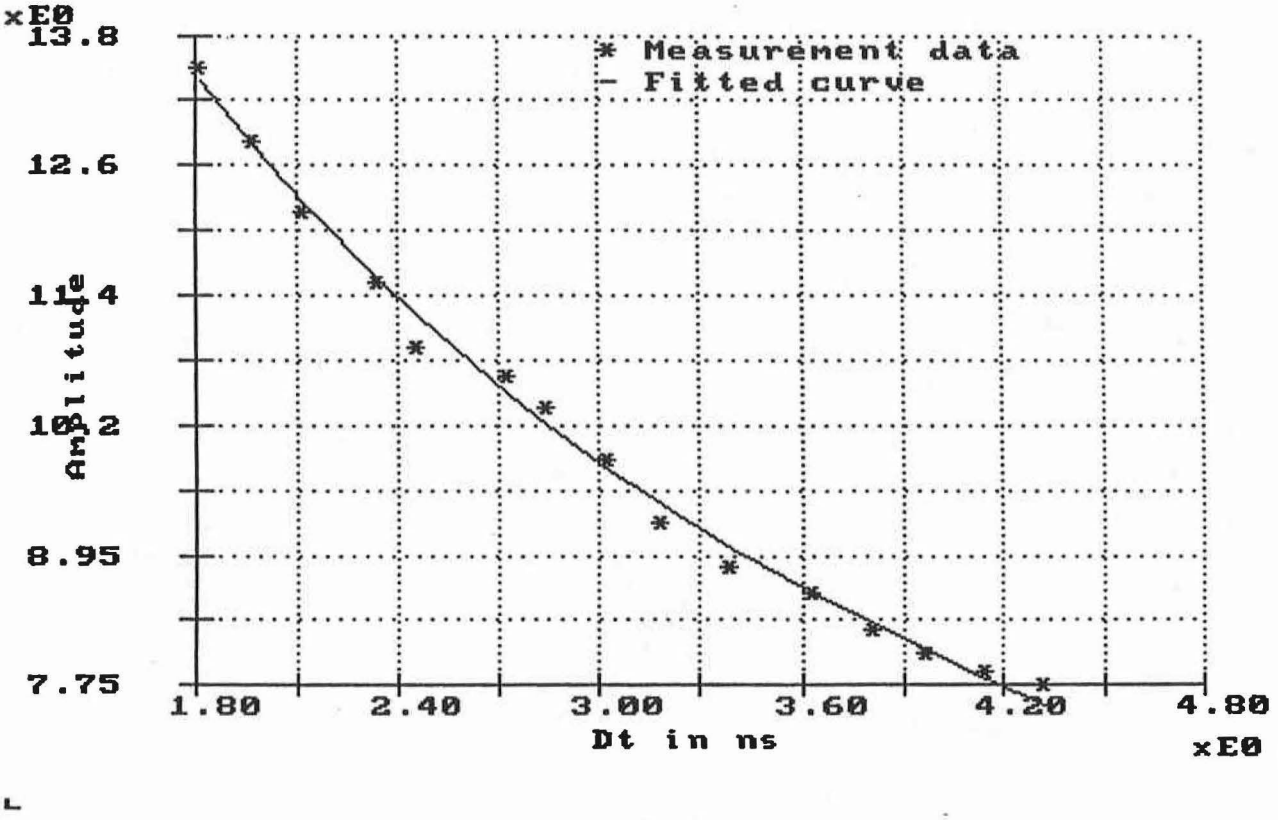

Figure 12. Height Calibration Curve. Metal Plate Amplitude in Volts versus Time of Travel from the Tip of the Antenna to the Metal Plate (and back). Used to Adjust Calculation for Antenna Bounce.

between amplitude A and D_t (time between end reflection and peak) is of the form

$$A = b/(a + D_t) \quad (5)$$

the constants a and b were found from curve fitting to be 1.4678 and 43.832 respectively.

b) Speed Calibration

It has been reported by Canadian researchers (Chung and Carter, 1991) that the surface echo voltage amplitude varies with the speed of the vehicle and that the speed of data acquisition should be limited to less than 3 mph. This conclusion conflicted with earlier TTI work reported in Study 930-5F in which reasonable estimates of surface thickness were obtained from GPR waveforms collected at speeds of both 5 and 40 mph.

To evaluate this further, tests were conducted on a very large sheet of aluminum foil (10 ft x 5 ft), with the long dimension in the direction of travel. GPR vehicle speed was varied from 0 mph to 45 mph. For each test the time between the end reflection and surface echo (D_t) was computed, the end reflection was subtracted and the amplitude of reflection was computed for the middle of the foil. The results are shown in Table 2.

Table 2. Influence of Vehicle Speed on GPR Amplitudes.

Speed (mph)	Amplitude (volts)	D_t (nanoseconds)	Adjusted Amplitude
0	11.32	1.95	11.32
15	11.42	1.94	11.41
25	11.48	1.96	11.49
35	11.15	1.94	11.14
45	10.95	2.04	11.27

The final column is the amplitude adjusted for bounce, using the D_t values and Equation 5. The amplitudes were adjusted to that of the static condition with a D_t of 1.95 nanoseconds. The D_t in the 45 mph test was 2.04

nanoseconds, indicating a higher antenna than the other speeds (around 1.95 ns). The adjusted amplitudes are similar, indicating little or no major influence of speed on the amplitude of reflection.

2.4 System Performance Tests

As part of this research project the TxDOT requested the development of a set of GPR performance criteria. These criteria are to be used in purchasing new GPR systems and to provide a baseline for evaluating the performance of new GPR currently under development. The following four performance criteria were recommended. They are based on performance monitored with the Penetradar's GPR and TTI data acquisition and processing system.

a. Signal to Noise Ratio Test (Clutter)

The antenna is mounted at its operating height (10-14 inches) above a minimum 16 square foot (4' x 4') metal plate. The radar unit is turned on and allowed to operate for 10 minutes. After warm-up, the system is operated at maximum pulse rate and a single radar waveform is recorded. The end reflection is also recorded and subtracted from the metal plate reflection using the techniques described in Section 3 of this report. The signal to noise ratio is described by the following equation:

$$\frac{\text{Noise Level}}{\text{Signal Level}} < 5\% \qquad (6)$$

where

Signal Level is defined as the metal plate amplitude of reflection (volts) measured from peak to the preceding minimum.

Noise Level is defined as the maximum amplitude (volts) of any peak occurring between 2 and 10 ns after the metal plate reflection.

The Noise to Signal test results for the GPR unit should be less than 5%.

b. Signal Stability Test (Jitter)

The same test configuration is used as described in the noise/signal test. Fifty waveforms are recorded at the maximum data acquisition rate, no less than 25 waveforms/second. The signal stability is evaluated using the following equation:

$$\frac{A_{max} - A_{min}}{A_{avg}} < 1\%$$

where

A_{max} is the maximum amplitude for any of the 50 recorded waveforms

A_{min} is the minimum amplitude for any of the 50 recorded waveforms

A_{avg} is the average amplitude for all 50 waveforms

The signal stability test results for the GPR should be less than 1%.

c. End Reflection Test

The same test configuration and results from the noise/signal ratio tests should be used. The amplitude of the end reflection directly preceding the metal plate reflection is measured. The size of the end reflection should be:

$$\frac{A_E}{\text{Signal Level}} < 50\%$$

where

A_E is the amplitude of end reflection in the 4 nanosecond window preceding the surface echo.

The end reflection in the metal plate test should be less than 50% the amplitude of metal plate reflection.

d. Concrete Penetration Test

The antenna is placed at its operating height above a six inch thick concrete slab which is sitting on a large metal plate. The slab is at least 36" x 36", non-reinforced with a minimum age of 28 days. The amplitude of reflection for the top and bottom of the concrete slab is measured. The concrete Penetration Test is defined by the following equation:

$$\frac{A_{bottom}}{A_{top}} > 25\%$$

where

A_{top} is defined as the amplitude of reflection from the surface;

A_{bottom} is defined as the amplitude of reflection from the metal plate beneath the concrete.

The Penetration Test results for the GPR should be greater than 25%.

3. DESCRIPTION OF DATA ACQUISITION AND PROCESSING SYSTEM

3.1 Introduction

The TTI software package provides the capability of both collecting GPR waveforms at user defined intervals along the highway and of using signal processing techniques to interpret these recorded waveforms. In the data acquisition mode, the GPR triggers at 50 Hz or one trace every 20 msec. The user can either collect every waveform or specify the number of waveforms to be skipped prior to the acquisition of the next trace. In establishing the data acquisition scheme the first step is to establish at what interval GPR waveforms are required. For anomaly detection (such as voids or stripping) or short sections of highway, one waveform every foot may be required. For network level thicknesses inventories one waveform every 50 foot may be adequate. Typically, for network level applications, a vehicle speed of 40 mph has been used; for anomaly detection a speed of 10 mph has been used. Given the required sampling rate, the vehicle speed and the maximum rate of data acquisition, an appropriate field data acquisition rate can be computed.

The remainder of this section will discuss the data processing software.

3.2 Input Files

A standard record format is used for the files containing radar waveforms. Each record has 2048 bytes (1024 words). Words 1 through 1022 contain digitized voltages (0 to 4095) representing voltages from -10 to 10 volts. Words 1023 and 1024 contain the distance measuring information.

The three standard input files to the system are as follows:

*.DAT contains the collect GPR radar traces for the highway,

*.MTL contains the metal plate reflection waveform,

*.END contains the end reflection waveform.

These three files are required in all cases where layer thickness computations are to be made. A fourth file is needed for special applications in which the top layer is very thin or consists of multiple significantly different asphalt layers. With the 1GHz systems a reflection overlap will occur for any layers less than three inches thick. This overlap may contaminate both amplitude and time delay estimates. To address the overlap problem, a Template file is used which contains a representative

trace from a thick homogeneous asphalt layer. The use of template subtraction is described further in section 3.4 of this report.

3.3 Example of Layer Thickness Calculation

The basic operation of this module involves the user manually identifying peaks in a single data trace and setting windows about those peaks. The software then automatically locates peaks within the specified windows for every trace in the .DAT file and measures amplitudes and time delays. From these amplitudes and times the calculation of both a) the relative dielectric of each layer and b) the thickness of each layer is made using the equations given in Section 1.

As an example of the layer thickness computation, the GPR waveform from an asphalt test box is shown in Figure 13. The thickness of both the asphalt and granular base layer was 6 inches; the wooden box containing the sample was resting about 3 inches above the floor. Each sample is 30" x 30" x 12" contained within a plywood box. The corresponding GPR waveform, shown in Figure 13, has had the end reflection automatically removed. The large peak at 4 nanoseconds is from the surface; the next is from the top of the granular base. The negative peak just after 10 nanoseconds is where the wave enters air.

The waveform also shows the three user defined windows and the measured amplitudes and time delays. In the metal plate test an amplitude of reflection of 12.92 volts was recorded. The computation of dielectrics and layer thicknesses proceeds as follows:

Using Equation (1)

$$\sqrt{\epsilon_{ac}} = \frac{A_m + A_o}{A_m - A_o} = \frac{12.92 + 5.25}{12.92 - 5.25} = 2.369$$

Using Equation (2)

$$h_{ac} = 5.36 \frac{x\Delta t}{\sqrt{\epsilon_{ac}}} = \frac{5.36 \times 2.64}{2.369} = 5.98''$$

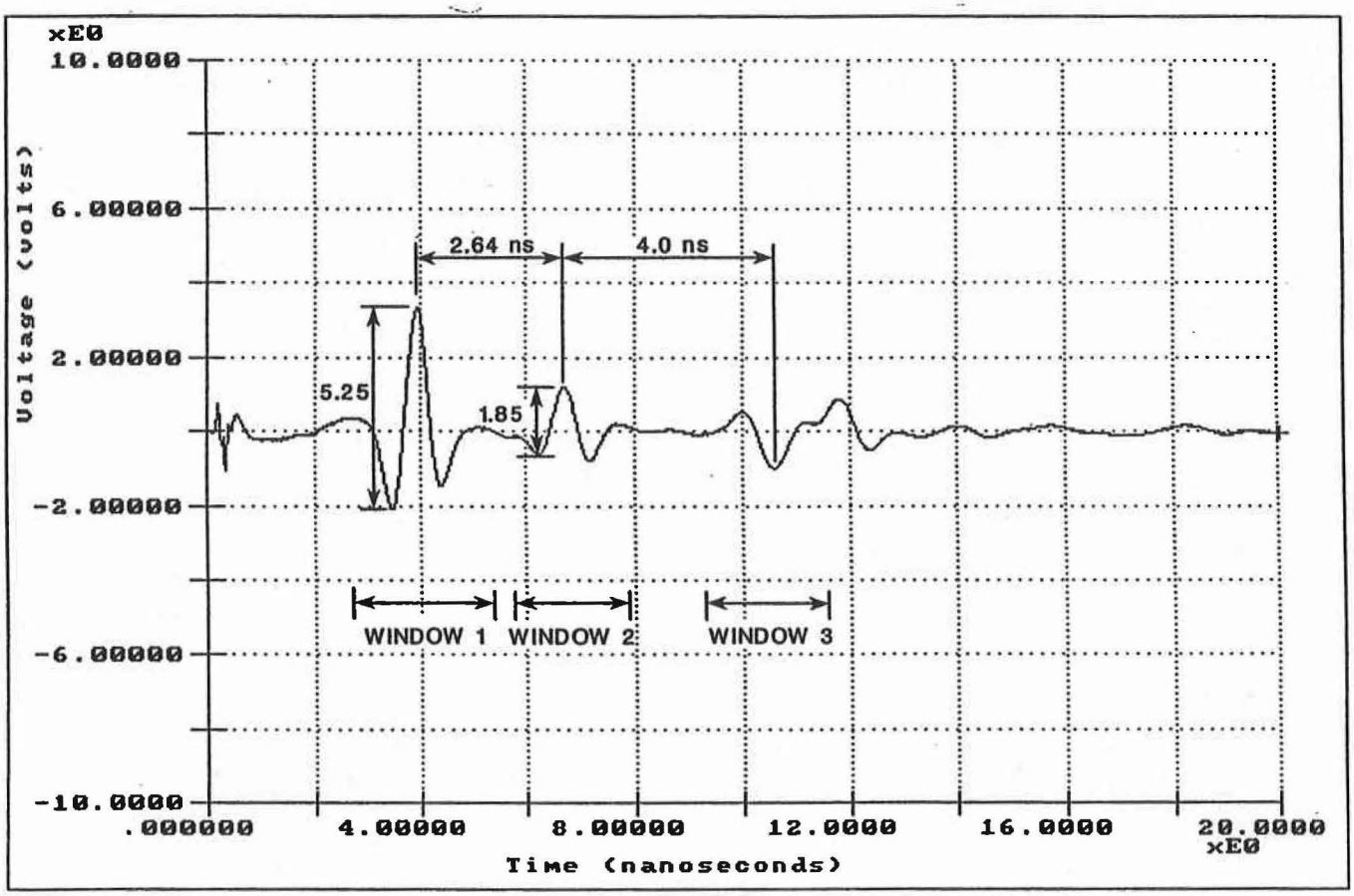

Figure 13. Example Layer Thickness Computation.

Using Equation (3)

$$\sqrt{\epsilon_b} = \sqrt{\epsilon_a}\left[\frac{1 - \left(\frac{A_o}{A_m}\right)^2 + \left(\frac{A_1}{A_m}\right)}{1 - \left(\frac{A_o}{A_m}\right)^2 - \left(\frac{A_1}{A_m}\right)}\right]$$

$$= 2.369\left[\frac{1 - \left(\frac{5.25}{12.92}\right)^2 + \left(\frac{1.85}{12.92}\right)}{1 - \left(\frac{5.25}{12.92}\right)^2 - \left(\frac{1.85}{12.92}\right)}\right]$$

$$= 3.349$$

Using Equation (2)

$$h_{base} = 5.36x\frac{\Delta t}{\sqrt{\epsilon_b}} = \frac{5.36 \times 4}{3.349} = 6.40''$$

The calculated thickness of the base (h_{base}) includes the thickness of the wood at the bottom of the test box.

The above example was presented to summarize the layer thickness calculation performed within the system. The software contains many options to assist in tracking peaks and handling the thin layer problem. Typical screens from the system are presented in the next section.

3.4 Description of Data Processing Software

The main screen in the data processing and reporting system is shown in Figure 14. The first five options of this screen are used in processing the waveforms. The last three-parameter display, color map and statistical computing are outputs and will be discussed later. Each of the five available data processing options are discussed below.

a) Option 1 Select/Change File Names

When selected, Figure 15 is displayed, and the user specifies the names of the files containing the GPR waveforms to be processed.

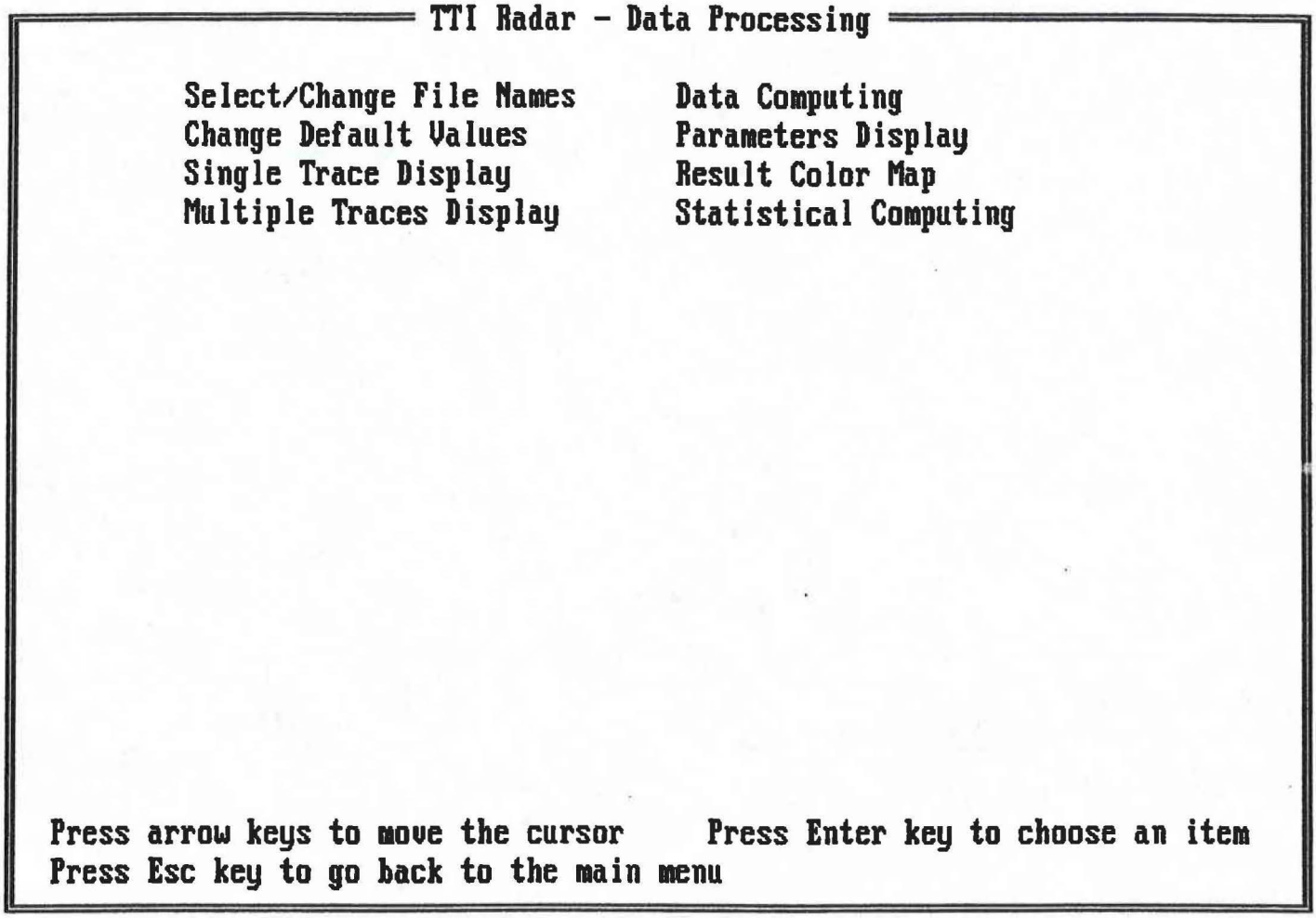

Figure 14. GPR Data Processing System. Main Menu Screen.

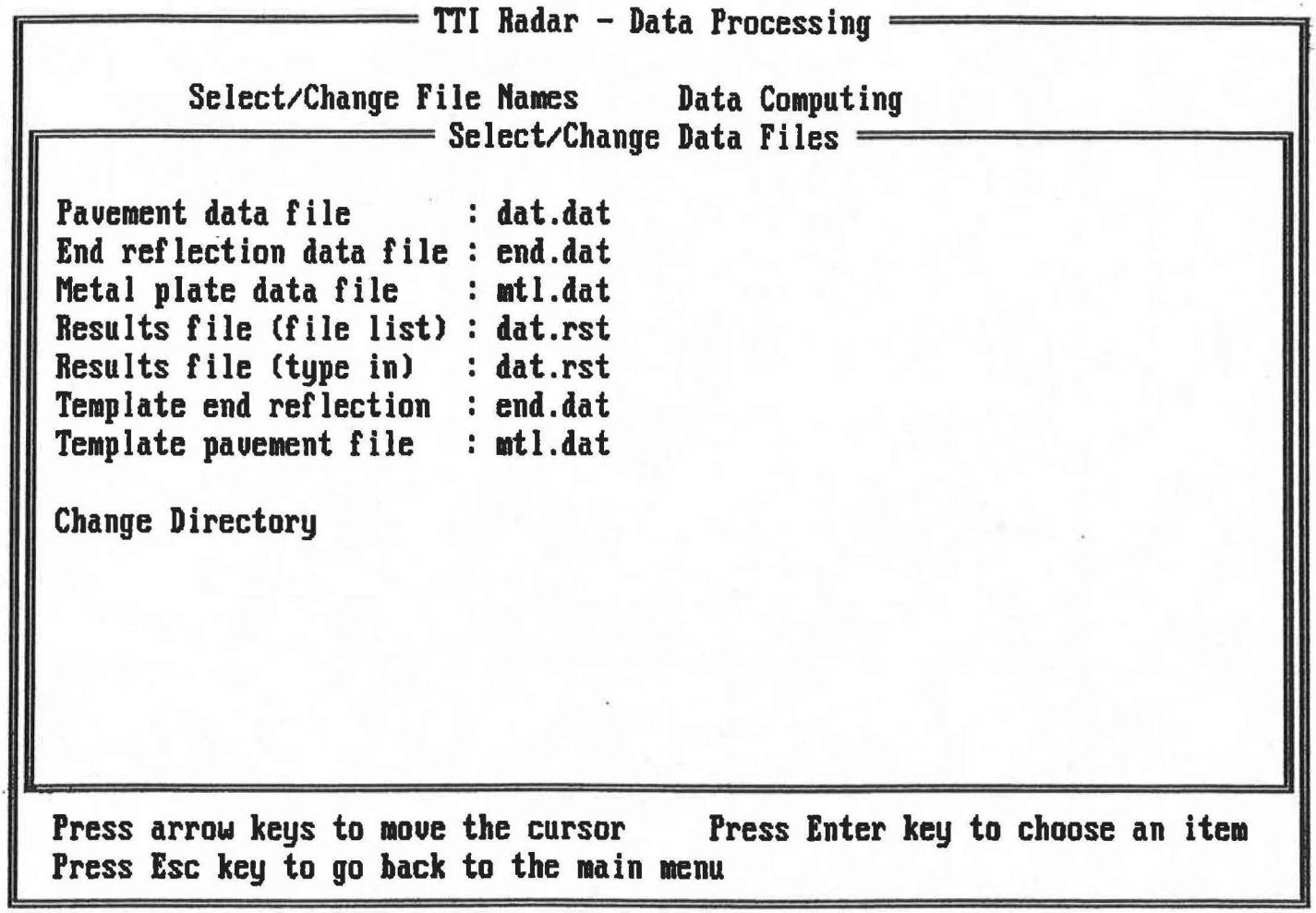

Figure 15. GPR Data Processing System - File Selection Menu.

b) Option 2 Default Values

When selected, Figure 16 is displayed, and the user has several options, the most important of which are described below.

Remove End Reflection. As mentioned previously, every waveform collected has the antenna end reflection superimposed upon the beginning of the waveform. Figure 9 shows the metal plate reflection with end reflection. Figure 10 shows the end reflection obtained by pointing the antenna to the sky. When this option is selected, the software aligns and automatically subtracts this end reflection. Figure 17 shows the results of subtracting the end reflection from Figure 9. It is worth noting that after subtraction very little noise is present in the waveform and the legs of the surface echo are symmetrical. End reflection subtraction is automatically applied to the metal plate waveform. The user has the option of removing the end reflection prior to any waveform display or processing. Normally the end reflections are removed prior to processing.

Velocity Factor. This is the time calibration factor collected after data acquisition as shown in Figure 11.

Remove Template. (Remove Surface Echo). This option is specified to minimize problems caused by thin surfacings in which reflection overlaps can make true peak detection difficult. This option is demonstrated in Figure 18, which shows the GPR waveform from a thin surfacing (2 inches) on top of a granular base. As can be seen, there is some overlap between the reflection from the surface and that from the top of the base in the original trace. In selecting this option the user must also input a template file on the Select/Change File Name menu (Figure 15). This file contains a waveform collected on either a thick asphalt surface or the metal plate reflection. It is the shape of the reflected waveform which is important. In applying "Remove Template", the waveform from the specified template file is aligned, scaled and subtracted from the surface echo containing the known signal overlap. The resulting waveform after subtraction is shown in Figure 18; the residual trace is compared with the input waveform. Amplitude and time calculations are performed on the waveform after subtraction. The template subtraction permits the amplitude of the reflection from the top of the base to be more clearly determined.

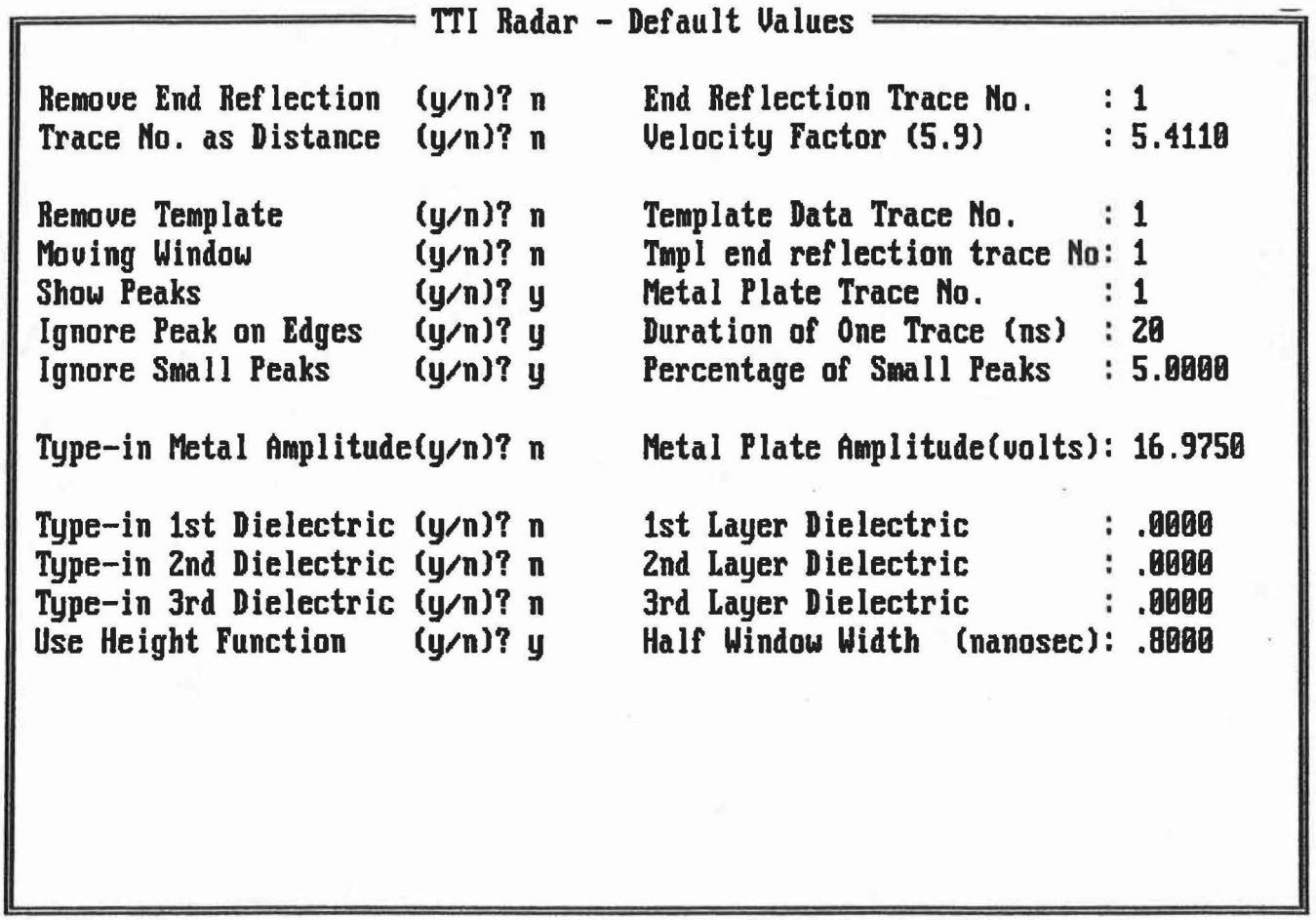

Figure 16. GPR Data Processing System - Default Values Menu.

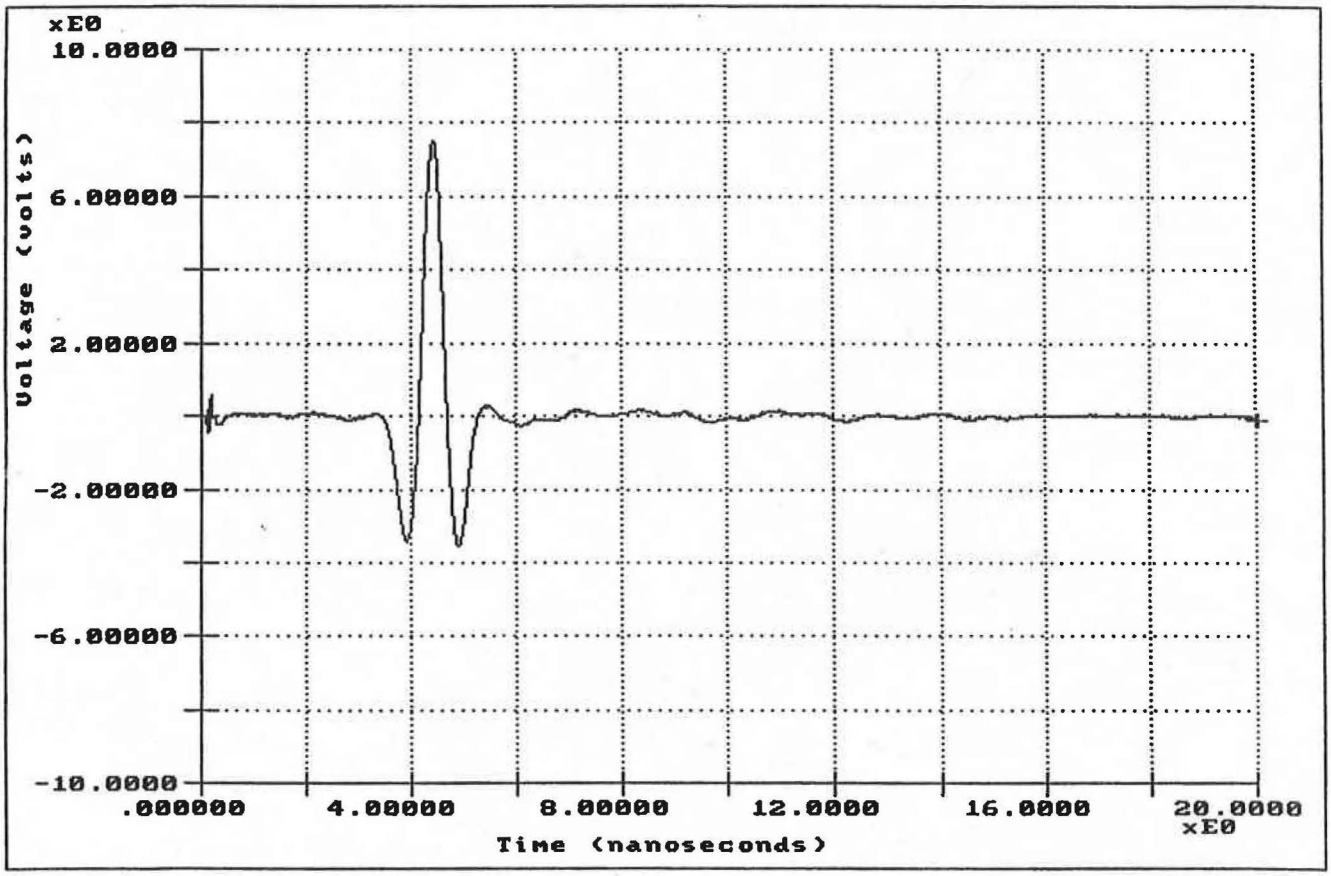

Figure 17. Metal Plate Reflection with End Reflection Removed.

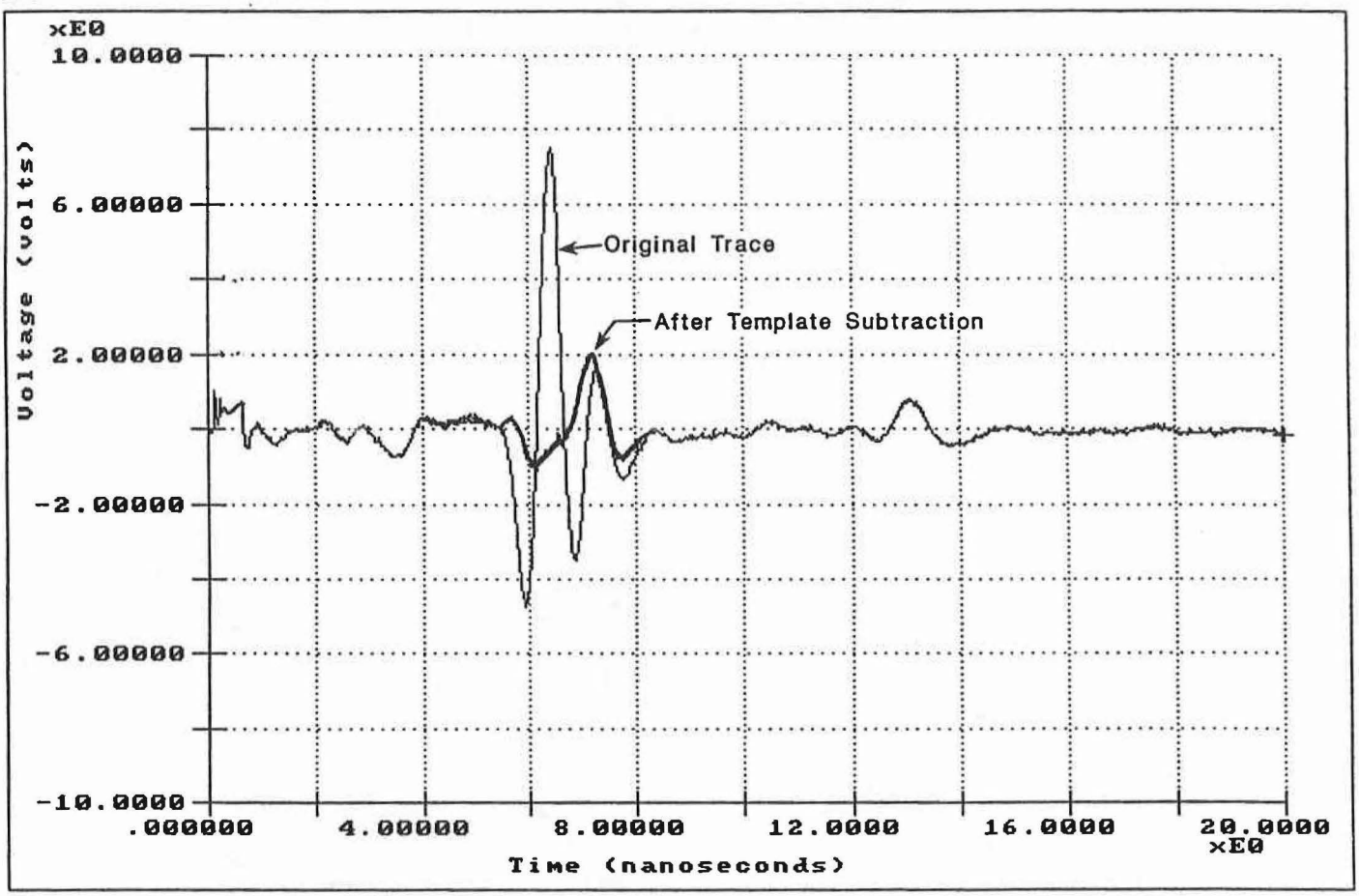

Figure 18. Example of Template Subtraction. The Thin Surface (2 inches) Causes Reflection Overlap at Surface.

Moving Window. As shown in Figure 13, the user has to specify windows in which the software will search for peaks which represent layer thicknesses. In some instances, when the layer becomes considerably thicker such as at a localized level up, the reflection from the top of the base may move outside of the specified window. When selecting the moving window option, the window is automatically adjusted to center around the last peak found. As the time location of the peak changes the search window will also change.

Show Peaks. During Data Computing (to be described later), if this option is chosen, the software places a (+) in each window identifying the peak located. This is a useful option just to be sure that the correct peak is being tracked.

Ignore Peaks on Edges. This option tells the system to ignore peaks found at the edge of the search windows. In this case, both the time and amplitude from the previous waveform will be used when processing the current waveform.

Ignore Small Peaks. This option tells the system to ignore all peaks whose amplitudes are less than a user specified percentage of the surface echo. Five (5%) percent is usually the minimum threshold specified. Below this level it is difficult to determine if the peak is actually a layer interface reflection or system noise. If the peak is less than that specified the amplitude and time from the previous waveform will be used when processing the current waveform.

Type-in Dielectrics. Provides the user with the option of overwriting the calculated layer dielectrics.

Use Height Function. Permits the user to correct for antenna bounce. This option was discussed earlier. It uses the height calibration curve shown in Figure 12.

c) Option 3 Single Trace Display

A single GPR run may collect several thousand waveforms. This option permits the user to display any single waveform. All of the waveforms presented in this report were obtained using this option, for example, see Figures 9 and 10.

d) Option 4 Multiple Trace Display

This option permits the user to stack multiple GPR traces along the highway. An example is shown in Figure 19, this being for an eight inch asphalt layer on top of a seven inch base. The vertical axis shows distance along the highway.

e) Option 5 Data Computing

This is the option in which the user defines the windows for a specific waveform and identifies which waveforms are to be processed. A typical set-up screen is shown in Figure 20. In this example the user specified 2 windows, window 1 from 4 to 8 nanoseconds, window 2 from 8 to 12 nanoseconds. The peak is defined as the amplitude from the maximum to either the preceding or trailing minimum. The "side" option permits the user to select either preceding (1=Left) or trailing (2=Right) minimum. The peak can also be either a positive or negative as specified in the "peak" option. All traces or a subset of traces can be selected for processing. The Default values specified, such as time calibration factor, moving window, etc., are applied during the data processing.

Once the Begin-Compute is selected the peaks in each window are located and the dielectric and thicknesses for each layer are computed. The results are stored in the output file specified in the Select/Change File Name option. The output file is given the extension .RST.

3.5 Data Outputs

The results stored in the .RST file can be output using either the parameter display, statistical computing options, or color map output. Each will be described below.

a) Parameter Display

The results stored in the .RST file include up to 4 amplitudes (representing the surface and three subsurface reflections), 3 time delays (travel times through 3 pavement layers), 3 layer dielectrics and 3 thicknesses. The first output of this system is a graphical display showing the variations in any of these parameters along the highway.

Two examples of graphical outputs are shown in Figures 21 and 22. Figure 21 shows the variation in asphalt thickness along a 300 ft. length of highway. Figure 22 shows the variations in amplitude of reflection from the bottom of a concrete slab from US59 in Houston. This 10 inch jointed

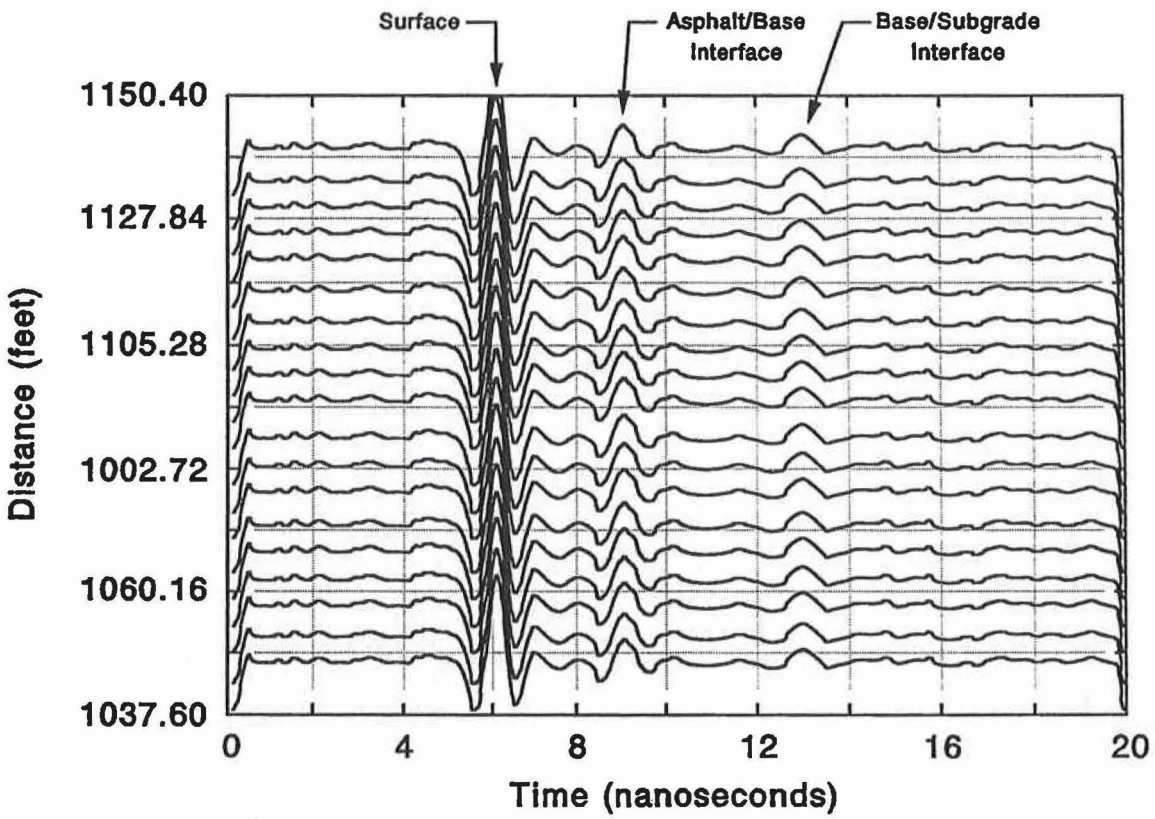

Figure 19. Multiple GPR Traces taken Along a Highway.

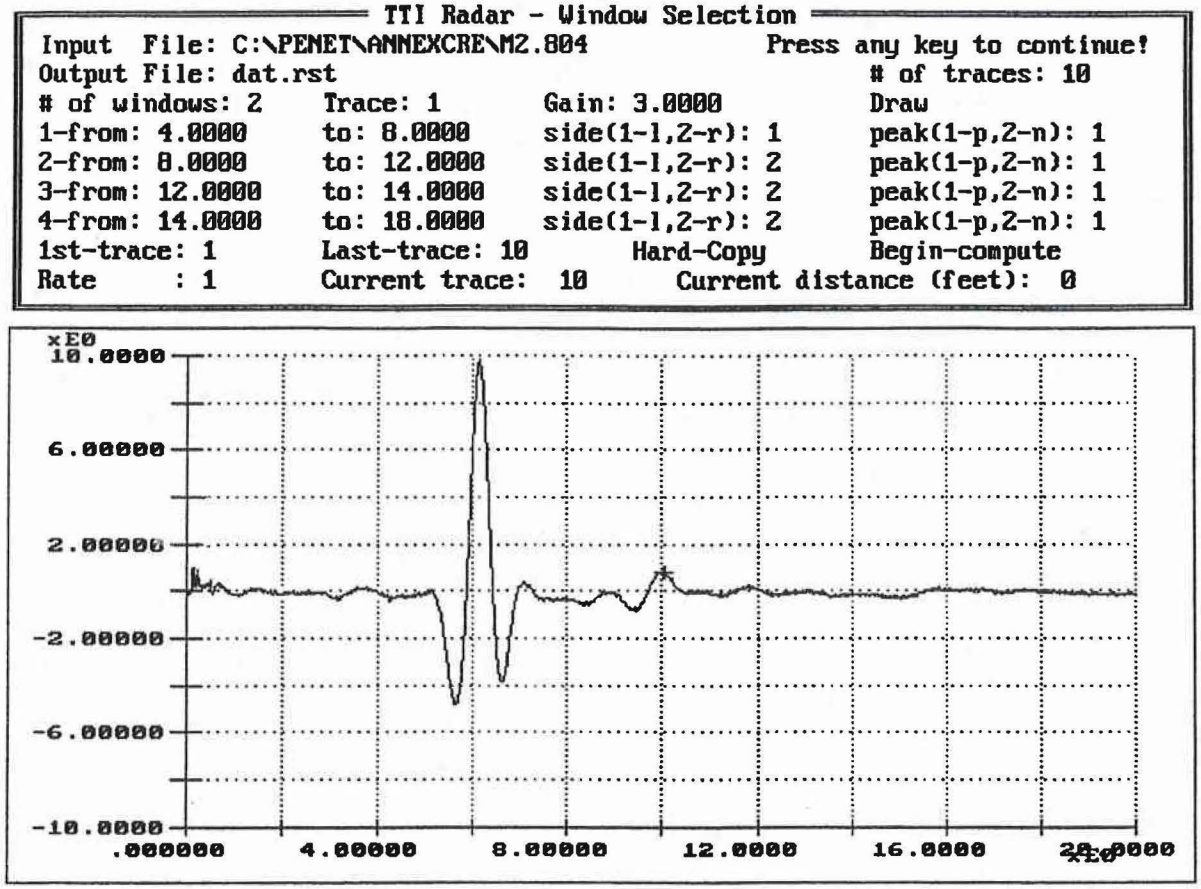

Figure 20. GPR Data Processing System - Data Computing Screen.

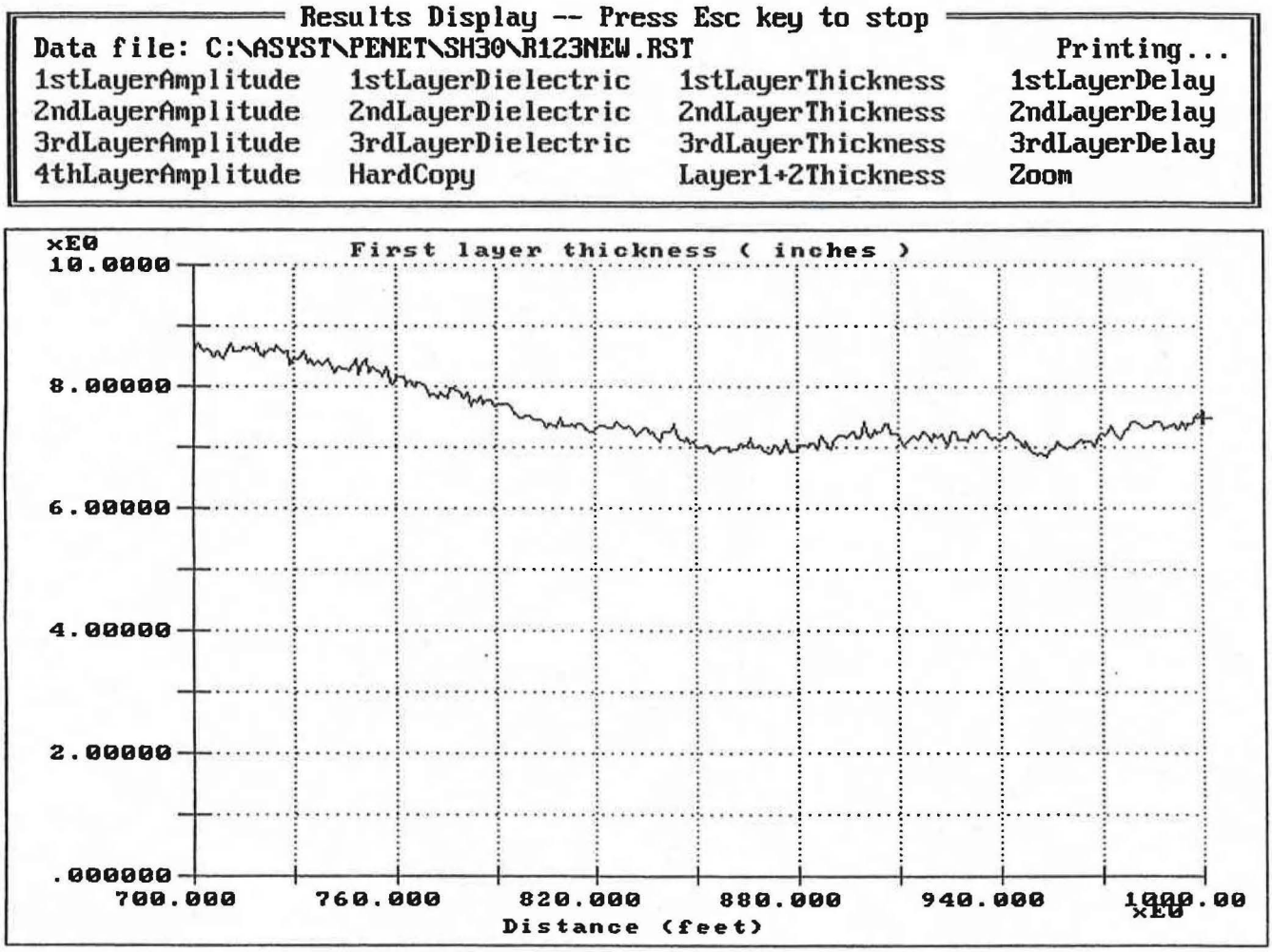

Figure 21. GPR Data Processing System - Parameter Display Output. Layer Thickness Computed along a Highway.

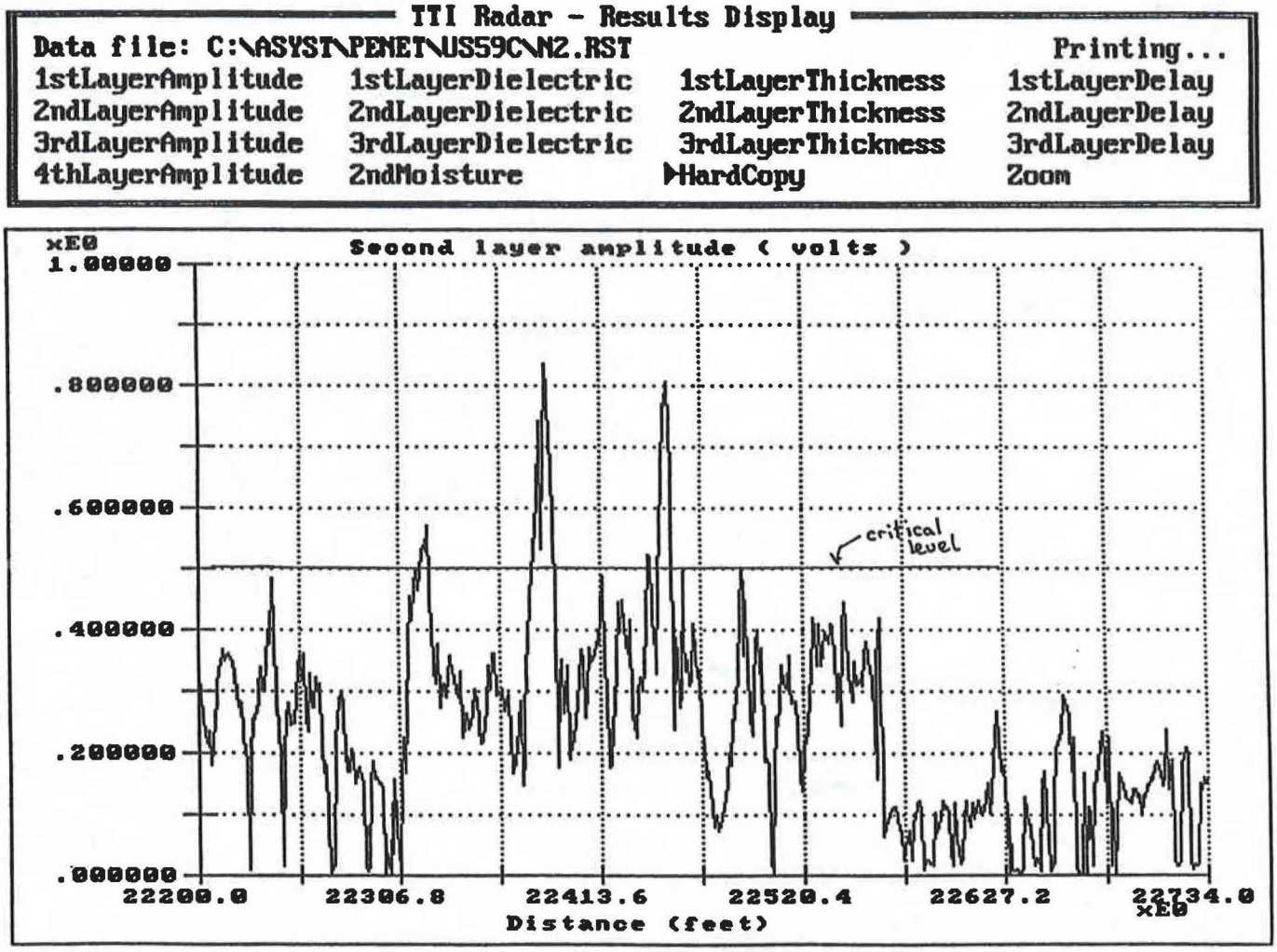

Figure 22. GPR Data Processing System - Parameter Display Output. Amplitude of Base Reflections Computed along a Highway.

concrete slab had water filled voids beneath the slab. A critical amplitude level was established at 0.5 volts by testing the slab in a location known to have water filled voids. Figure 22 was used to successfully locate moisture filled voids. Void detection activities will be discussed later.

b) Statistical Reports

A frequent requirement in interpreting GPR results is to be able to scan along the highway and identify locations meeting certain criteria. For example, find all locations where base dielectric is greater than 10 or all locations where the amplitude of reflection from layer 2 is greater than 0.5 volts. The amplitude of reflection is frequently used to identify potential subsurface moisture problems. The user may wish to extend the criteria by finding locations that exceed a certain criteria on at least 3 consecutive GPR traces. In the statistical computing option the user sets such criteria and receives a tabular output of locations meeting the criteria. The set up screen for running this option is shown in Figure 23. The system automatically generates the mean, low and high value of each of the parameters stored in the .RST file. The user then sets the criteria of interest. In this figure the specified criteria are layer 2 dielectrics of greater than 10 and less than 50 on at least 3 consecutive traces. Sections of highway meeting this criteria will be output in table form.

c) Color Map Output

This option provides a color representation of surface and base thickness along a highway. The output is directed to the screen where the surfacing is colored in red, the base is colored in yellow. A representation of this output is shown in Figure 24.

d) ASCII File Output

The .RST file containing location, amplitudes, dielectrics, time delays and thicknesses can only be used within the system software. A utility has been included to convert the format to ASCII standard format. The converted file can be read by any spreadsheet for additional processing and graphical output.

	Low	High	Statistics		
			Mean	Low	High
Amplitudes					
Peak 1	>	<	4.62	4.51	4.73
Peak 2	>	<	1.21	1.00	1.57
Peak 3	>	<	0.82	0.15	0.97
Peak 4	>	<	0.15	0.06	0.32
Dielectrics					
E1	>	<	5.6	4.8	7.5
E2	>10	<50	9.1	5.9	13.2
E3	>	<	12.1	6.0	17.5
Thicknesses					
H1	>	<	4.3	3.6	7.2
H2	>	<	10.9	8.7	12.3
H3	>	<	12.0	10.0	16.5
Consecutive	03				

Figure 23. GPR Data Processing System - Statistical Report Set Up Screen.

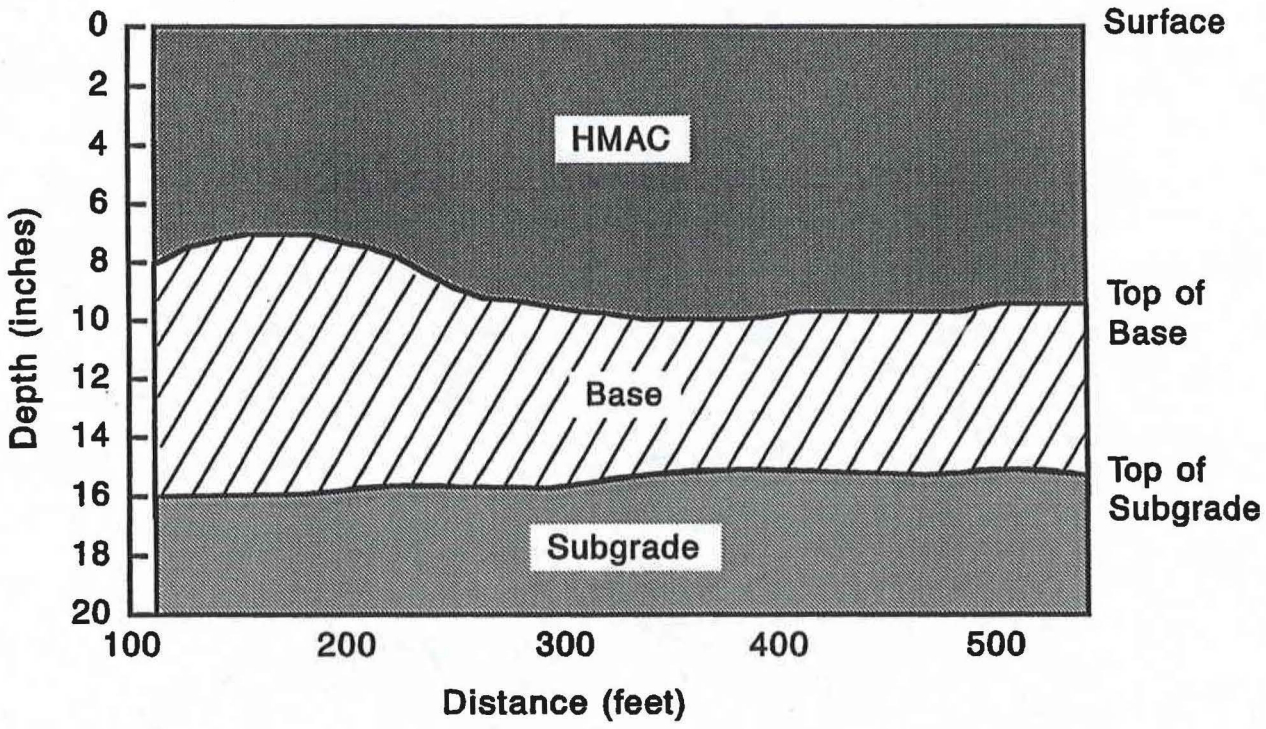

Figure 24. GPR Data Processing System - Color Map Output Showing Surface and Base Thicknesses along a Highway.

4. CASE STUDIES

This section presents the results of several GPR surveys conducted for the TxDOT. The hardware and software described in the earlier sections of this report were used to collect and process the GPR waveforms. Where possible, ground truth testing was performed to validate the GPR predictions.

Case 1. Layer Thickness Measurements - US 82 District 1

Background

The section of US 82 runs from the intersection with FM 1417 near Sherman to Sadler approximately 10 miles to the west. The highway was constructed in 1973 as a 4 lane divided highway with a pavement structure consisting of 6 inches of flexible base, 8½ inches Black Base and a 1½ inch Hot Mix surfacing. This 10 mile section is a candidate for rehabilitation. As shown in Figure 25, the existing surface has extensive block cracking and several sections have poor ride.

A Falling Weight Deflectometer survey was scheduled by TxDOT Pavement Design Section as part of their routine pavement evaluation. However, one major concern was that of surface layer thickness. Several level up and overlays had been placed in some locations on the highway. As TxDOT wished to perform modulus backcalculation, what thickness should be used to process the surface deflection data? In lieu of taking cores at every 0.1 mile interval, the FWD test frequency, it was decided to use GPR for the layer thickness evaluation.

Survey Results

A GPR survey was conducted in October 1992; data was collected at 40 mph in both east and west bound directions. The data acquisition system was set up to collect one GPR trace for every 10 foot of pavement. Approximately 5900 GPR traces were collected in each run. Three typical GPR waveforms from US 82 with end reflections removed are shown in Figure 26; these are from the areas where calibration cores were taken. The results of the calibration tests will be described in the next section. From Figure 26 the waveform from core 5 was in an area where no level ups had been performed. This waveform represents the original pavement structure. Cores 3 and 4 were in areas where level ups had taken place; the bottom of the asphalt moves towards the right indicating longer travel times and thicker

Figure 25. Photograph of US 82 west of Sherman, Texas, Part of the 10 Mile Section Being Evaluated for Pavement rehabilitation. This Section is the Original Surfacing, Now 20 Years Old.

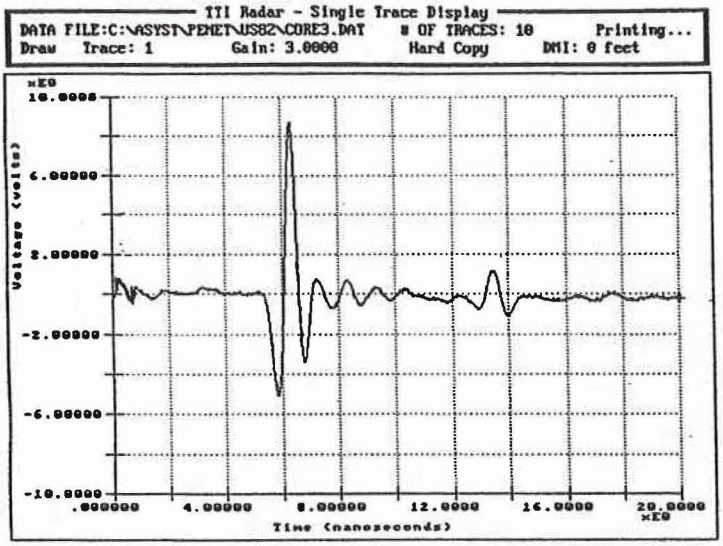

a. Core Hole 3

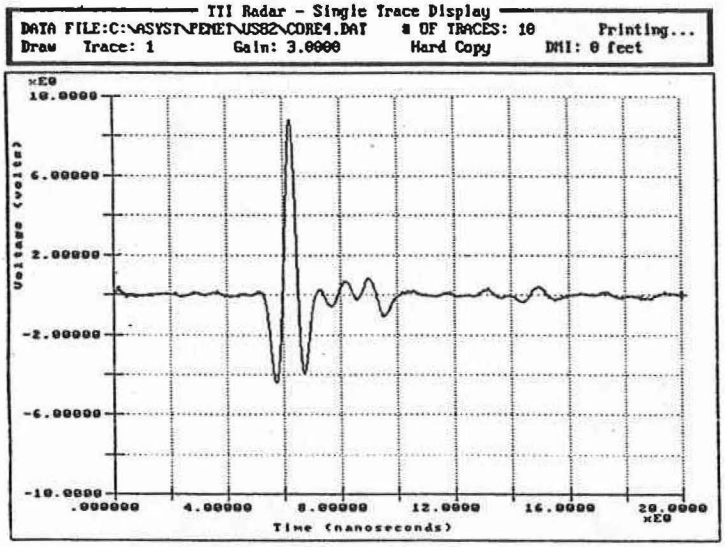

b. Core Hole 4

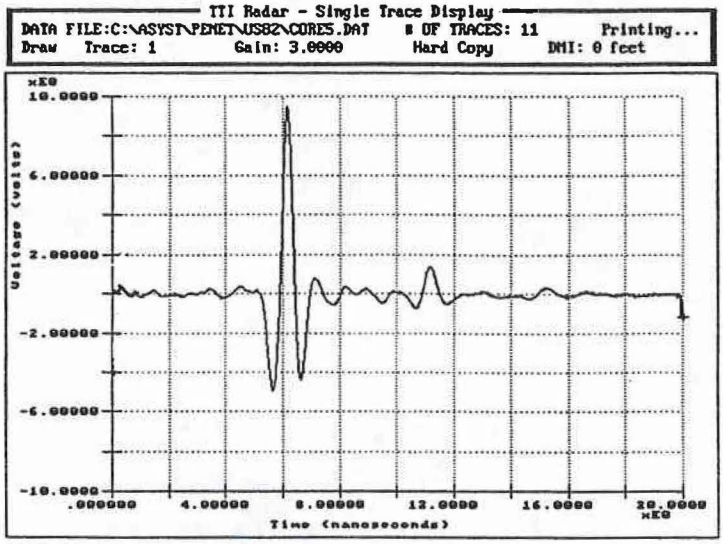

c. Core Hole 5

Figure 26. GPR Traces Obtain at Calibration Locations on US 82-District 1.

layers. Also intermediate reflections are found around 8 nanoseconds indicating distinct layering within the asphalt layer.

The GPR waveforms for the entire 10 miles were processed using the software described in section 3 of this report. The layer thickness predictions from two sections of the westbound run are shown in Figures 27 and 28. Figure 27 shows the first three miles of the westbound run. In this section the layer thickness remained relatively constant between 10 and 12 inches of asphalt. This section is the original construction prior to any level up work. Figure 28 shows the asphalt thicknesses from 4.7 to 6.2 miles from the beginning of the job. In this section, multiple level ups have been applied. The asphalt thickness ranged from 10 to 20 inches. In processing the entire 10 miles, sections of asphalt as thick as 24 inches were predicted.

Validation of Layer Thickness Predictions

To validate the asphalt thickness predictions three locations were selected. At each site a metal plate reflection was collected as well as a single GPR waveform from the pavement. Immediately after GPR testing a 4-inch core was taken at each location to verify thickness predictions. Figure 29 shows photographs of the field coring operation together with a photograph taken of the cores from each of the three locations. The GPR waveforms collected at each location were shown earlier in Figure 26. The core locations were identified as cores 3, 4 and 5. The thickness of the field cores was 14.75, 17.75 and 10.75 inches respectively. The processing of the GPR waveforms will be discussed in terms of thinnest to thickest.

Analysis of GPR Waveform from Core Hole 5

From Figure 26 the waveform from core 5 is the simplest to process. The surface echo is at 6 nanoseconds; the reflection from the top of the base is at approximately 11 nanoseconds. There are no distinct peaks between the surface and the base implying that the asphalt layer has a uniform dielectric with depth. Within the software two windows were set from 4 to 8 ns and 10 to 12 ns. The computed surface dielectric was 5.54 and computed surface thickness of 10.6 inches. This compares with the measured thickness of 10.75, which gives an error of 1.4%.

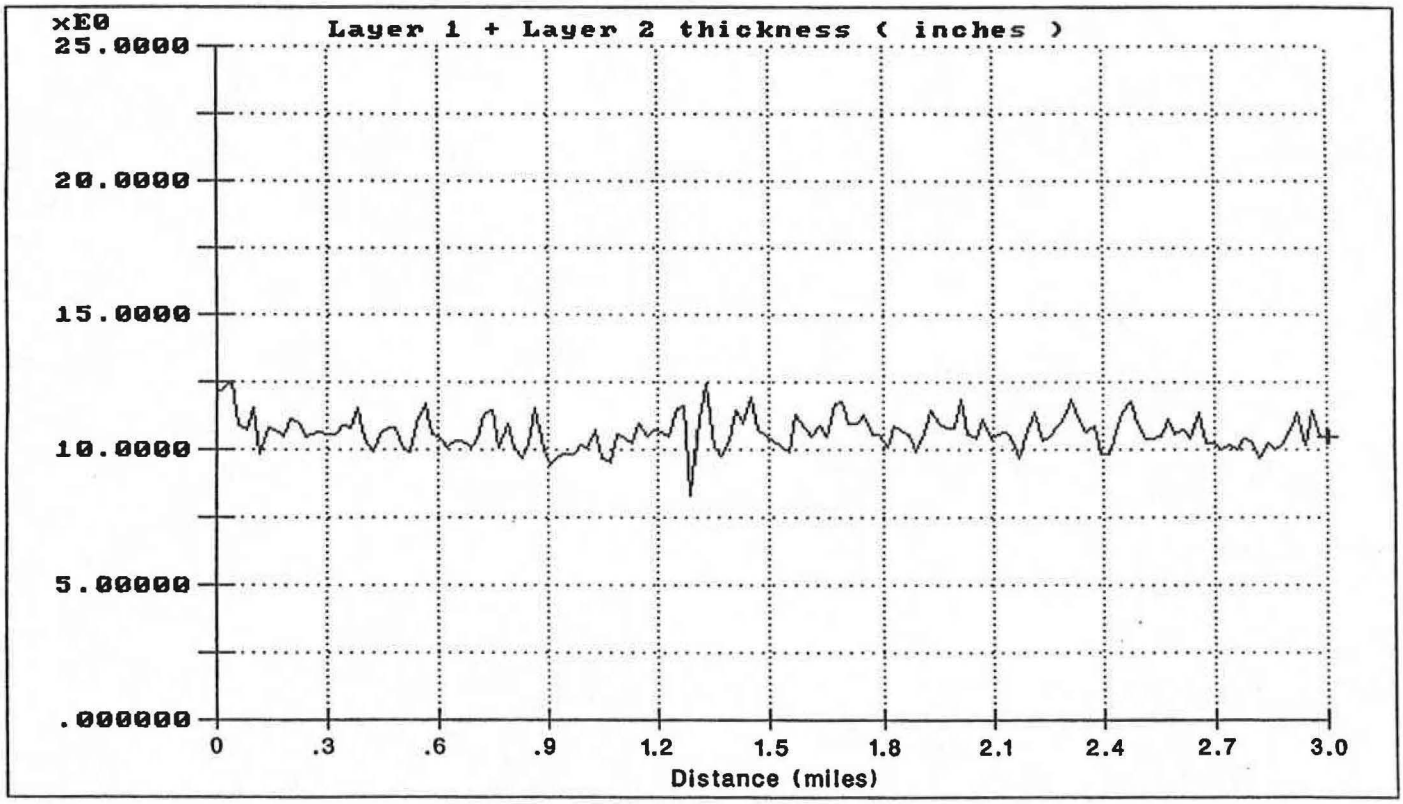

Figure 27. Asphalt Layer Thickness Predictions for US 82, Westbound from Mile 0 to 3.0 of Section.

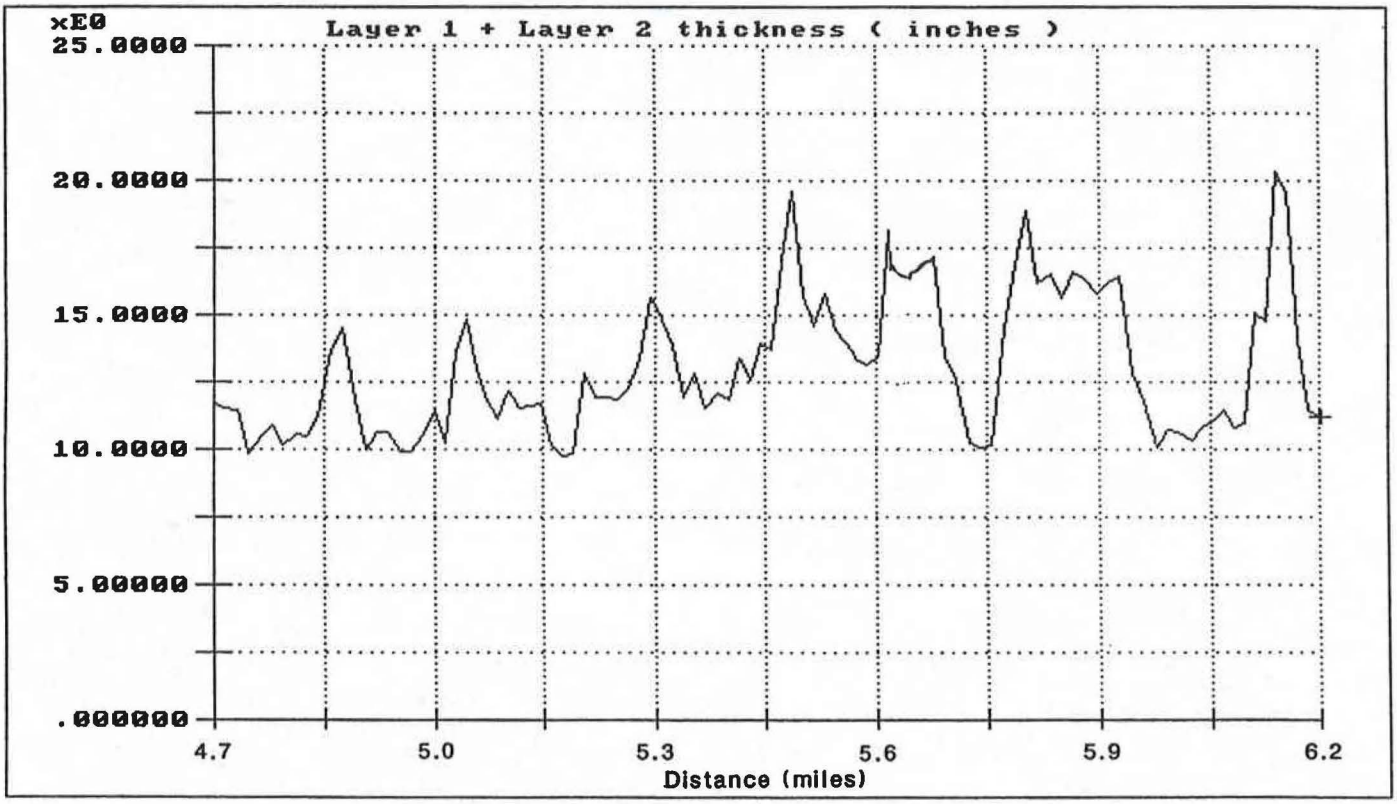

Figure 28. Asphalt Layer Thickness Predictions for US 82, Westbound from Mile 4.7 to 6.2 of Section.

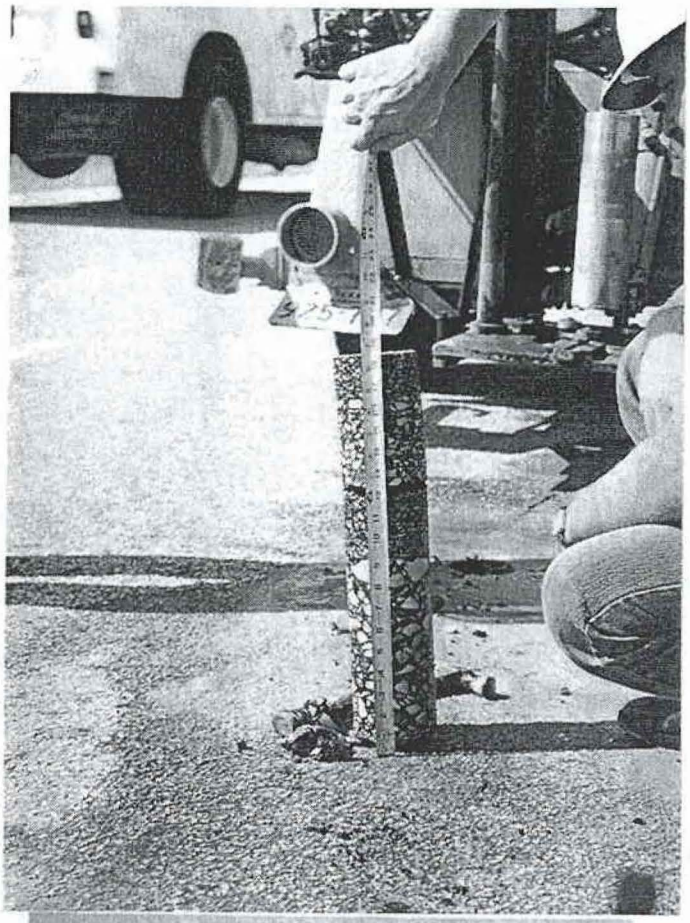

a) Field Validation

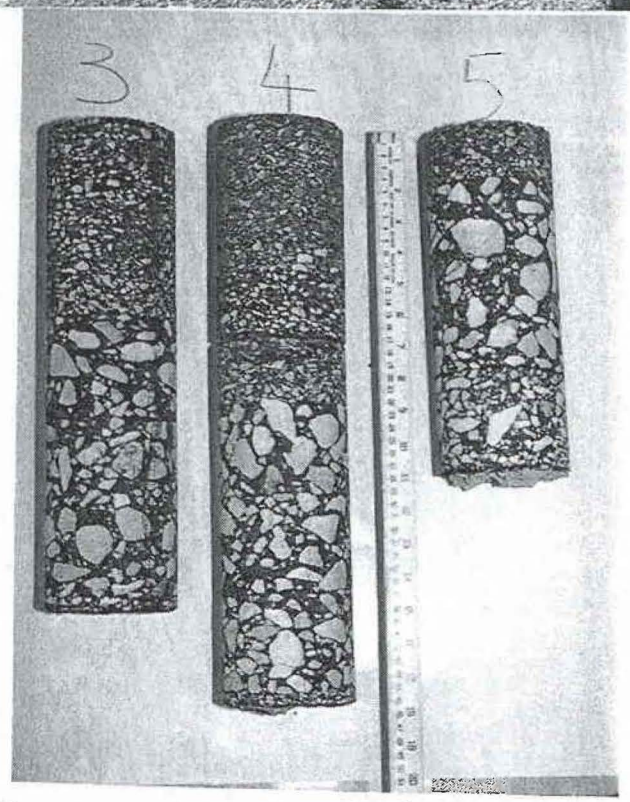

b) All Three Validation Cores. Core 5 is original thickness

Figure 29. Cores taken from US 82 near Sherman, Texas.

Analysis of GPR Waveform from Core Hole 3

From Figure 26 the waveform for core 3 has an intermediate peak at around 8 nanoseconds, indicating a change in dielectric for the lower asphalt layer. Two processing schemes were attempted. In the first the intermediate peak was ignored. This resulted in a computed dielectric of 4.87 and thickness of 16.2 inches, compared to the core thickness of 14.75 inches. In the second analysis, the asphalt was broken into two layers. The resulting dielectrics were 4.87 and 5.76 and asphalt thicknesses of 4.3 and 10.9, for a total asphalt layer thickness of 15.2 inches. The two layer analysis resulted in an error of layer thickness estimation of 3%.

Analysis of GPR Waveform for Core Hole 4

From Figure 26 the waveform from core 4 is the most difficult to process. The reflection from the top of the base is weak and located at approximately 15 nanoseconds. The one layer analysis technique resulted in an asphalt thickness prediction of 18.9 inches against the measured 17.75 inches.

The difficulty with this trace is the multiple reflections from the various level ups between 8 and 10 nanoseconds. The two layer analysis with an intermediate peak at 9 nanoseconds, resulted in dielectrics of 5.34 and 7.06, with thicknesses of 5.9 and 11.3 inches, giving 17.2 inches total (3.1% error). Just prior to 10 nanoseconds, there appears to be a negative peak which would indicate an asphalt layer of lower density (lower dielectric). Using a 3 layer model for the asphalt resulted in dielectrics of 5.34, 6.1 and 5.1 respectively, with asphalt layer thicknesses of 4.0, 2.8 and 12.1 inches (total 18.9 inches). The core itself did show evidence of a low density layer at approximately 7 inches below the surface; the core broke at that location. However, the low density layer is only two inches thick. The problem with the three layer thickness computation is that the low dielectric (5.1) was assumed to be representative of the material between the negative peak just prior to 10 ns and the reflection from the top of the base at 15 ns. This is not the case. The original asphalt layer (10 inches thick) is still in good condition. Additional analysis could be performed by adding more layers to the computation process, although this

is not warranted at this stage since the two layer model produced a reasonable error of 3.1%.

Summary of Layer Thickness Prediction on US 82

The GPR was found to have sufficient power to penetrate over 20 inches of asphalt. The one layer analysis was adequate where no level ups had been applied. The two layer analysis was needed wherever the level ups were found. From the three validation cores, the average error in predicting asphalt layer thickness was found to be less than 2.5%.

Case 2. Void Detection - US 59 District 12

Background

The site location is on US 59 just north of Humble, Texas in District 12. The pavement is 20 years old and consists of a 10 inch thick jointed concrete pavement over a six inch cement treated base. Dowelled joints were initially placed at 60 foot spacings with two sawed joints every 20 foot. The shoulders are asphalt and the total length of the project is 4.5 miles. The highway is four lanes divided with very heavy AADT and high truck percentages. The road is in generally poor condition. Faulting occurs in several places, some shattered slabs have been replaced and the overall ride of the section is poor (2.0 to 2.5). The highway is scheduled for reconstruction but not until 1997 or 1998. The District is interested in applying Concrete Pavement Restoration (CPR) techniques to the section to hold it until the reconstruction funds become available.

A major concern to the District was the pumping of subslab fines which were evident in several locations along the project. The District hoped that GPR could be used to locate subslab voids before undersealing.

GPR Test Program

To determine GPR ability to detect subsurface voids, a fifty slab test area was selected. Testing was conducted in the middle of a prolonged wet period, and it was known that the voids were moisture filled. In conducting the GPR survey, the antenna was mounted 9 inches above the surface to maximize the energy entering the pavement. Data was collected at approximately 10 mph with a waveform collected every foot.

Representative GPR waveforms for a void and no void location are shown in Figure 30. The concrete slab and cement treated base are very similar electrically. If the interface between slab and CTB is sound, then only a small amount of the GPR energy will be reflected, resulting in a small reflected peak. However, if a moisture filled void exists, then a substantial reflection will occur at the water surface. These are the two cases shown in Figure 30. The location of the slab/CTB interface was calculated by knowing the slab thickness and assuming a range of concrete dielectrics from 6 to 9. This means that the interface should occur somewhere between 4.8 and 6 nanoseconds after the surface echo. Stacked GPR

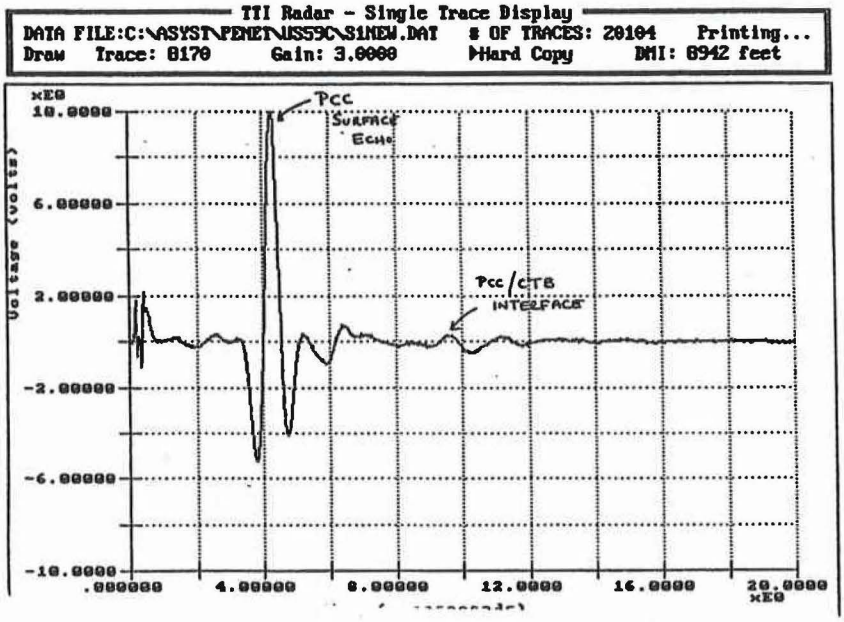

a. No Void Location.

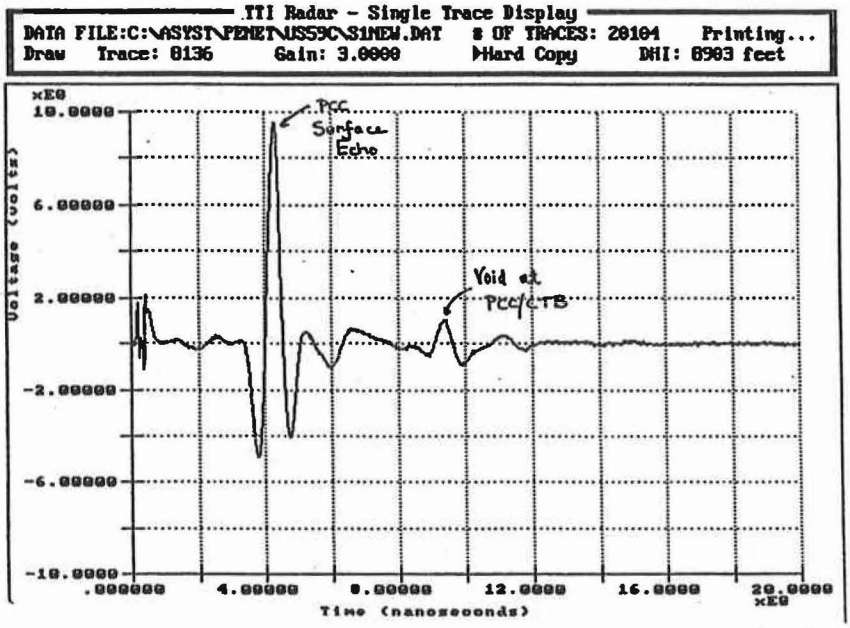

b. Potential Void Location.

Figure 30. GPR Waveform from US 59 Houston.

waveforms for a section of US 59 are shown in Figure 31; the potential moisture filled void location is marked.

In processing the GPR waveforms it was necessary to window into the slab/CTB interface and measure the amplitude of reflection along the highway. This is shown in Figure 32 and the location of 24 joints is sketched at the top of the figure. The amplitude of reflection varies significantly along the highway. The spikes in the amplitudes of reflection largely coincide with the joints in the pavement. The joints themselves were open, therefore a single spike at a joint was not a major concern as it would indicate a localized wet spot beneath the joint. However, in several locations, multiple adjacent traces were found to have high amplitudes of reflection.

In setting the criteria for void/no void, a critical voltage level has to be set. On this highway a location known to have a void was tested. At this particular location the seal between the concrete slab and shoulder had failed and water could be observed at the bottom of the slab. At this location, at the same antenna height an amplitude of reflection of 0.22 volts was measured. That voltage was used as criteria for void/no void areas in Figure 32.

Validation of Void Locations

Within the 50 test slabs, 5 joints were selected to run the epoxy core test developed as part of the Strategic Highway Research Program. Of these 5 locations, three were predicted by GPR to contain voids and two were predicted to have no voids.

The epoxy core test is shown in Figure 33. The first step is the drilling of a 1½ inch diameter dry hole approximately one foot from the joint. The hole is drilled about 14 inches in depth and compressed air is used to clean out the hole. A fluid epoxy mixed with food coloring is poured into the hole and allowed to set up overnight. The next day a standard 4 inch core is taken with the edge of the core being directly over the epoxy filled hole.

Two of the resulting cores are shown in Figure 34. Slab 6 was predicted to have a good interface whereas Slab 0 was predicted to contain a void. At Slab 0 the epoxy has flowed between the concrete slab and the CTB. On this particular core the top of the CTB had eroded, but in some

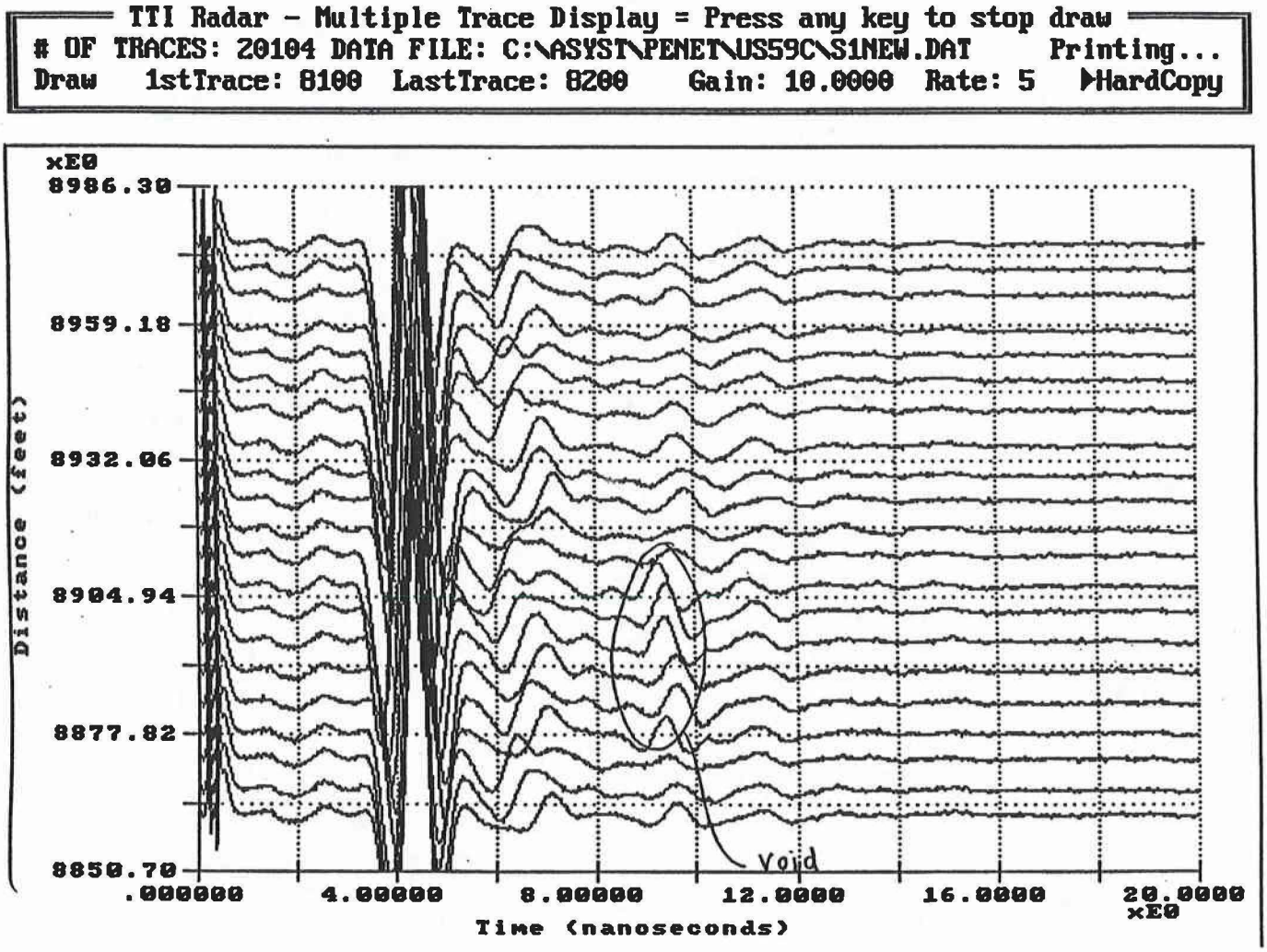

Figure 31. US 59 Southvoid - Multiple Traces used to Identify Void Length.

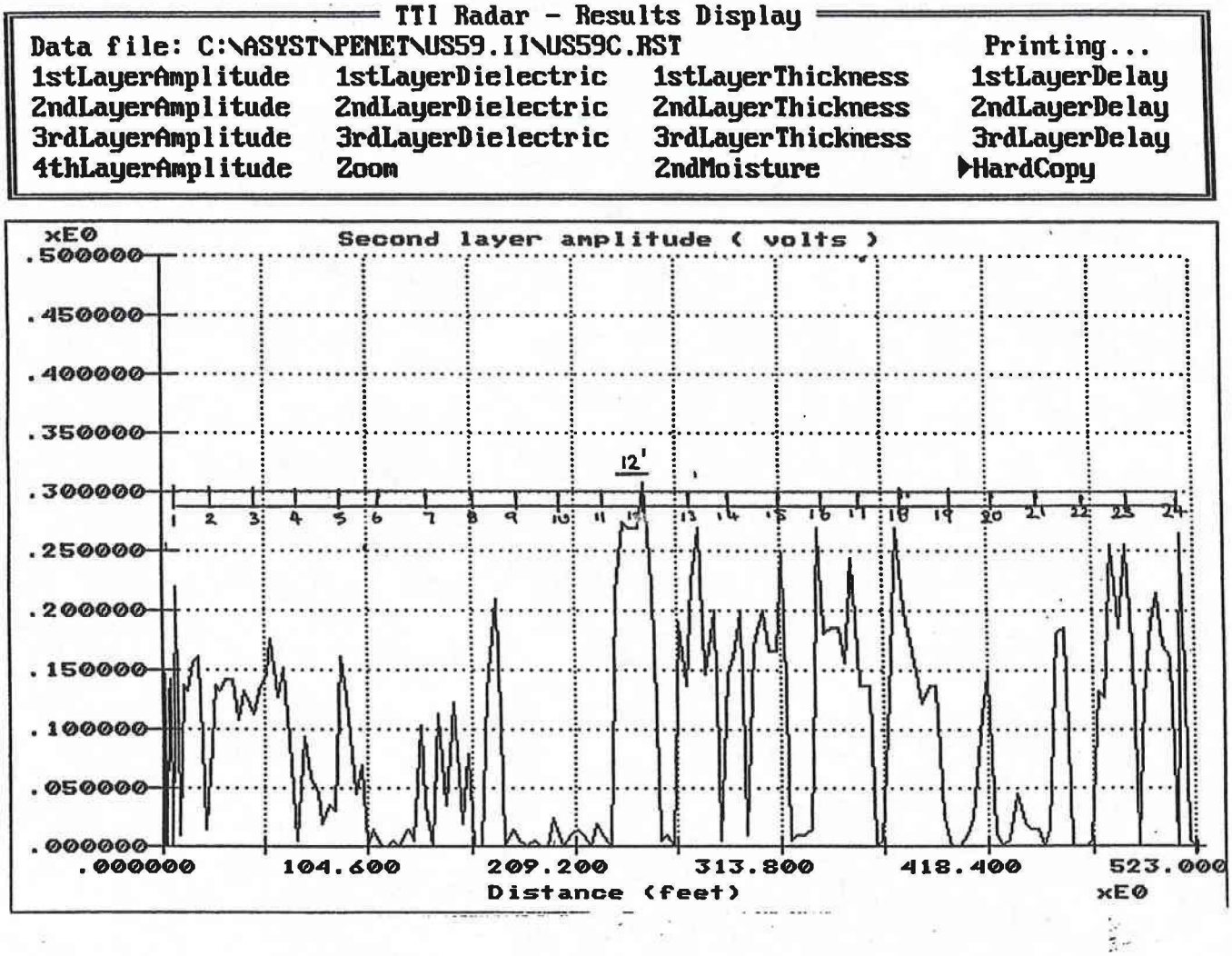

Figure 32. US 59 Amplitude of Reflection from Top of Base.

a) Drilling Dry Hole

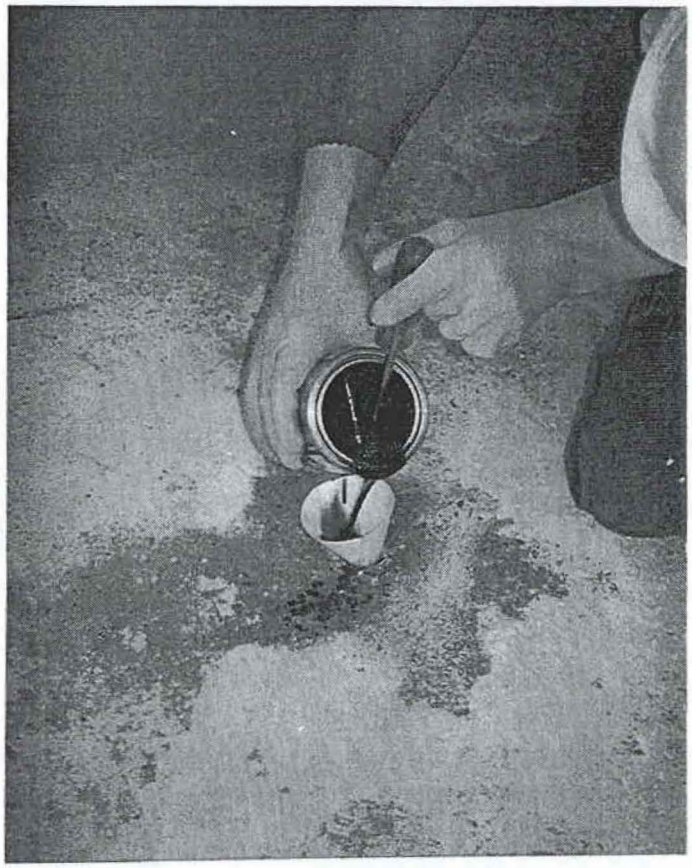

b) Pouring Fluid Epoxy
(contain red food coloring).

Figure 33. Epoxy Core Test on US 59.

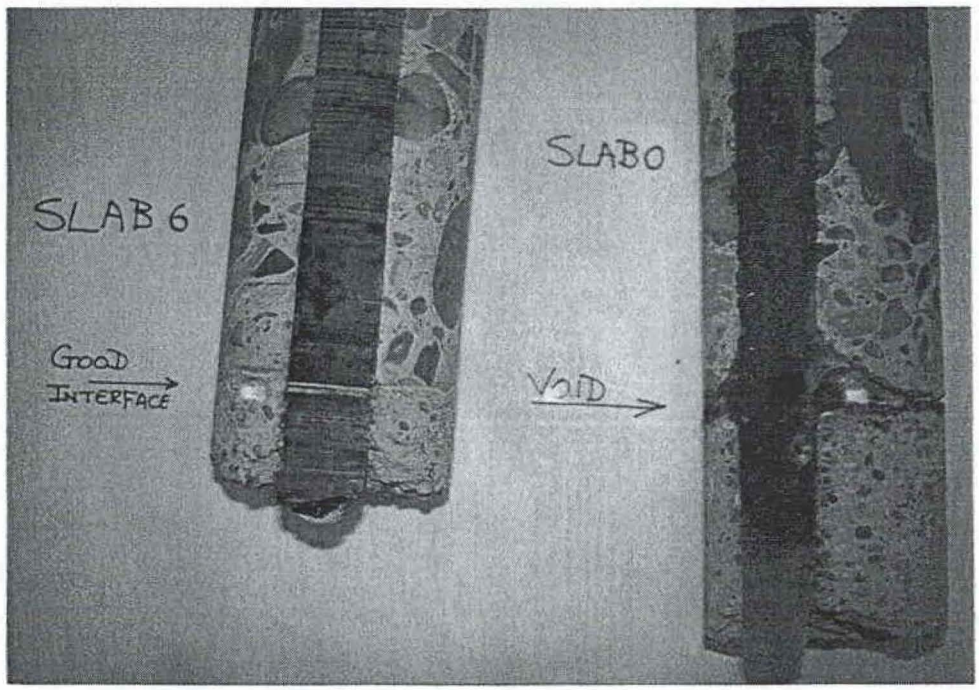

Figure 34. Results of Epoxy Core Test.

places there was still stone to stone contact. In all three predicted void locations moisture filled voids were found. The two no void locations were confirmed to have good bond between the slab and the CTB. Falling Weight Deflectometer tests were conducted over these joints. Various load transfer and void detection algorithms were used. None of the algorithms gave an indication of a problem with the thin void. The simple load transfer efficiency factor w_1/w_2 seemed to be the best void indicator when large voids were present.

Conclusions

These tests confirm that under certain circumstances GPR can be used to detect voids beneath concrete slabs. The conditions of this test were favorable to GPR, in that distinct voids were present and that they were moisture filled. Under these circumstances GPR could be used to detect even very thin voids (< 1/16 inch).

Whether GPR could be used to detect air voids is the subject of current research at the Texas Transportation Institute. Currently it appears that the GPR system will only be able to detect substantial air filled voids greater than ½ inch in thickness. It "probably" does not have sufficient power or resolution to detect air filled voids less than that thickness.

Case 3. Void Detection - IH 45 District 12

Background

Interstate 45 north of Houston consists of 4 to 5 inches of hot mix overlay on top of a 10 inch Continuously Reinforced Concrete Pavement. The pavement was experiencing problems in that localized wet spots would appear in the asphalt which would lead to potholing. The section was a maintenance headache primarily because the average daily traffic was in excess of 200,000 vehicles. The District suspected that voids had formed beneath the pavement trapping water. A GPR survey was requested to identify the subsurface problem. The section was scheduled for a milling and thin overlay, so a GPR survey was conducted during the milling operation. A photograph of the GPR test being conducted is given in Figure 35.

GPR Test Results

A short 500 foot section was selected for testing. A GPR survey was conducted collecting one trace for every foot. At the time of test, the structure consisted of two inches of asphalt (approximate), 10 inches of CRCP on a granular base. A typical GPR trace from this section is shown in Figure 36. The trace is fairly complex in that there is a thin asphalt overlay which causes some distortion between, 5.8 and 6.2 nanoseconds. The peak at eight nanoseconds is from the steel rebars at the middepth of the slab. The area of interest is the small peak just after 10.0 nanoseconds, this represents the interface condition between the bottom of the slab and the granular base.

As in other void studies the amplitude of this reflection was tracked over the test location. The variation in slab/base reflection amplitude is shown in Figure 37. The background amplitude is around 0.3 volts, however, between 230 and 290 feet the amplitude of reflection increases significantly. This increase means an increase in dielectric, which is associated with an increase in subslab moisture content. At position A the GPR trace shown in Figure 36 was obtained. This was thought to be an area with no subslab problems. The traces obtained from positions B and C are shown in Figure 38a) and b).

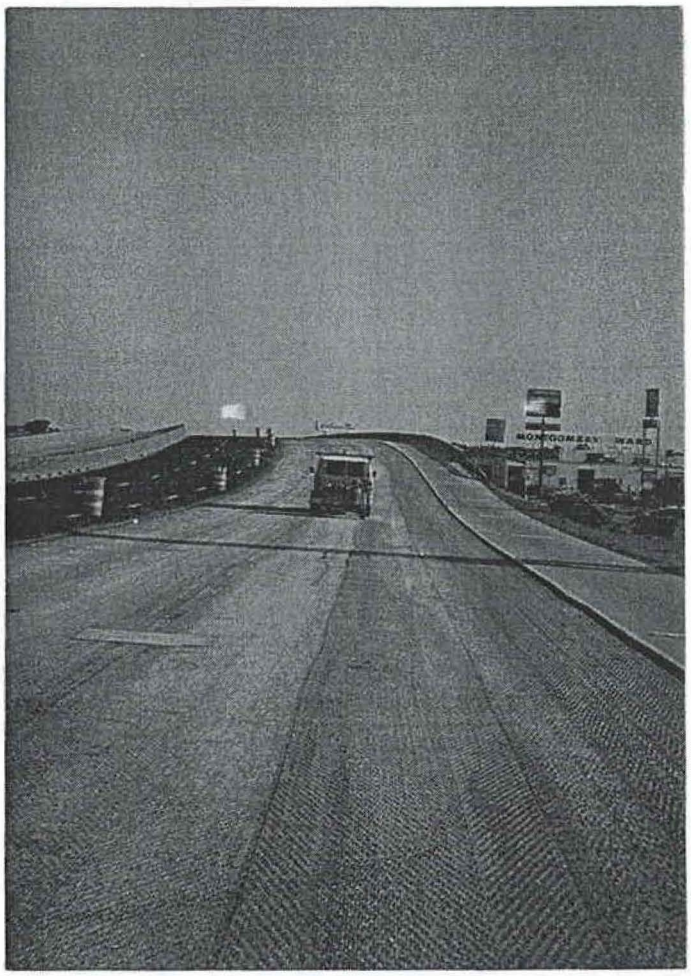

Figure 35. GPR Test of IH 45 North of Houston.

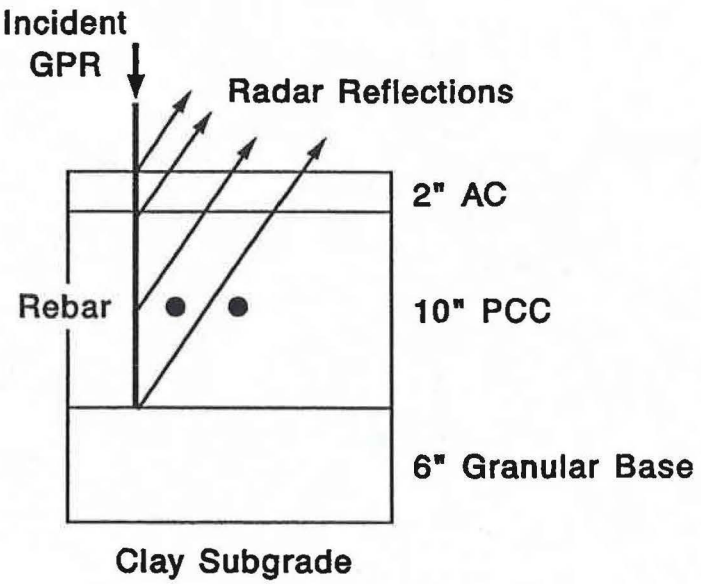

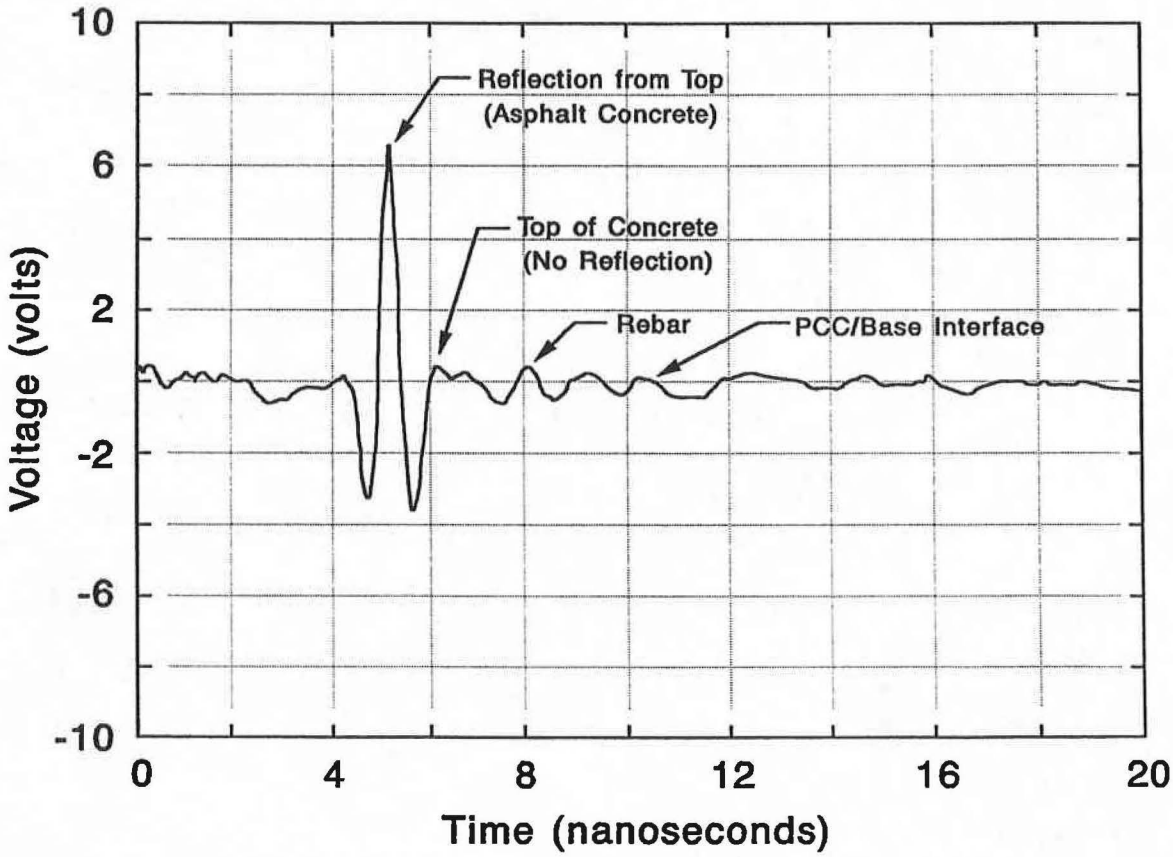

Figure 36. IH 45 Houston GPR Trace Obtained in a Location Where no Problems are Anticipated.

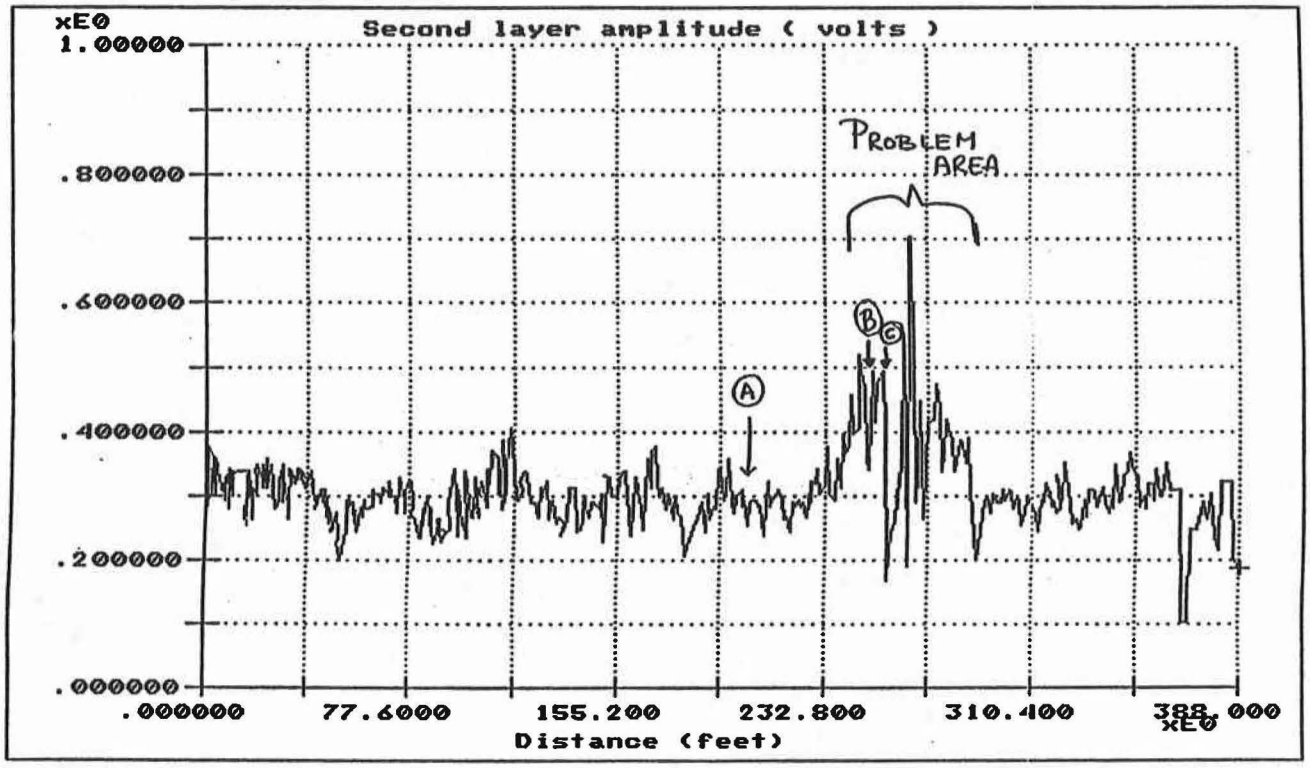

Figure 37. IH 45 Houston, Amplitude of Reflection from the Bottom of the Slab.

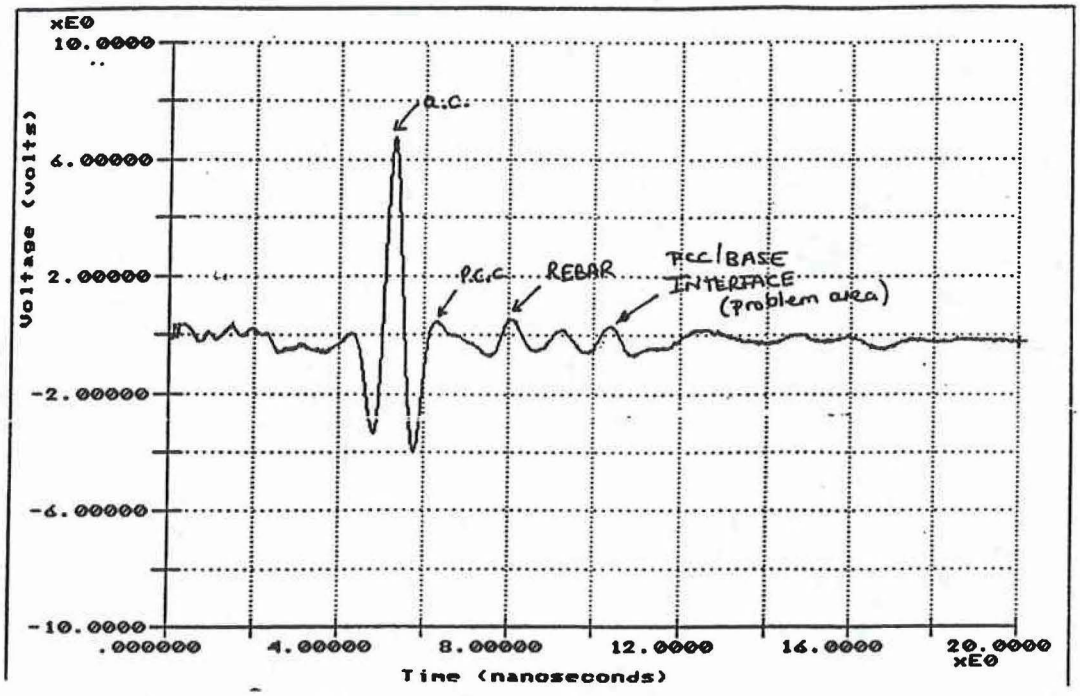

a. Location B, High Amplitude at PCC/Base Interface Indicates Moisture Problem Beneath the Concrete.

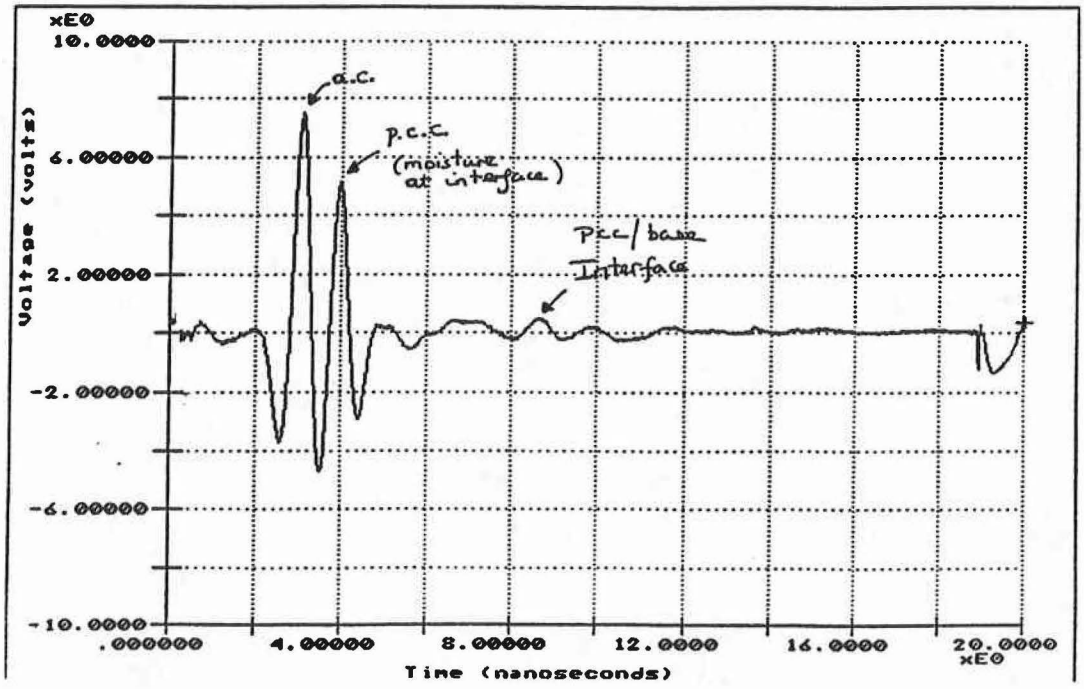

b. Location C, High Amplitude at AC/PCC Interface Indicates Moisture on Top of Slab.

Figure 38. IH 45 Houston GPR Traces Obtained from Suspected Problem Locations.

In Figure 38a an increase in the amplitude of the slab/base interface reflection is apparent. In Figure 38b the amplitude of asphalt/base interface becomes very large. The only explanation for this large peak in Figure 38b is moisture at the interface between the asphalt and concrete slab. No differences were observed from a visual evaluation of surface condition.

Ground Truth Testing

The purpose of this testing was to validate the subslab problems. Five test holes were drilled in the problem area identified in Figure 37. In all cases, when the hole entered the granular base water was found to enter the hole as shown in Figure 39. In several instances the water was observed to rise to about midslab depth (5 inches from the surface). Several of the holes were bailed out and in no instances were any voids found. The base beneath the slab appeared to be in good condition but clearly saturated with water under artesian pressure.

Conclusion

The problem beneath this pavement was not voids but trapped moisture. The locations where problems were found coincided with the low spots in the longitudinal profile. The water was entering at the bridge joints and other unsealed joints and draining beneath the slab to the low spots. The clay subgrade and impermeable shoulders meant that this water was trapped beneath the slab. Under the action of traffic this water was being forced through the cracks in the CRCP to the bottom of the asphalt overlay. Subsurface drains are now being considered to correct this problem.

On this job, the GPR was capable of detecting the wet spots beneath the concrete slab. However, GPR is not capable of distinguishing between a wet base and a moisture filled void. The user will need to apply judgement in interpreting GPR data. In all cases it is necessary to drill at least one pilot hole to validate GPR predictions. Whether the slab rests on a stabilized or unstabilized base is a major factor. In Case 2 the peaks were associated with voids at the top of an eroding cement stabilized base. In this case (of a granular base), they represent areas of trapped moisture.

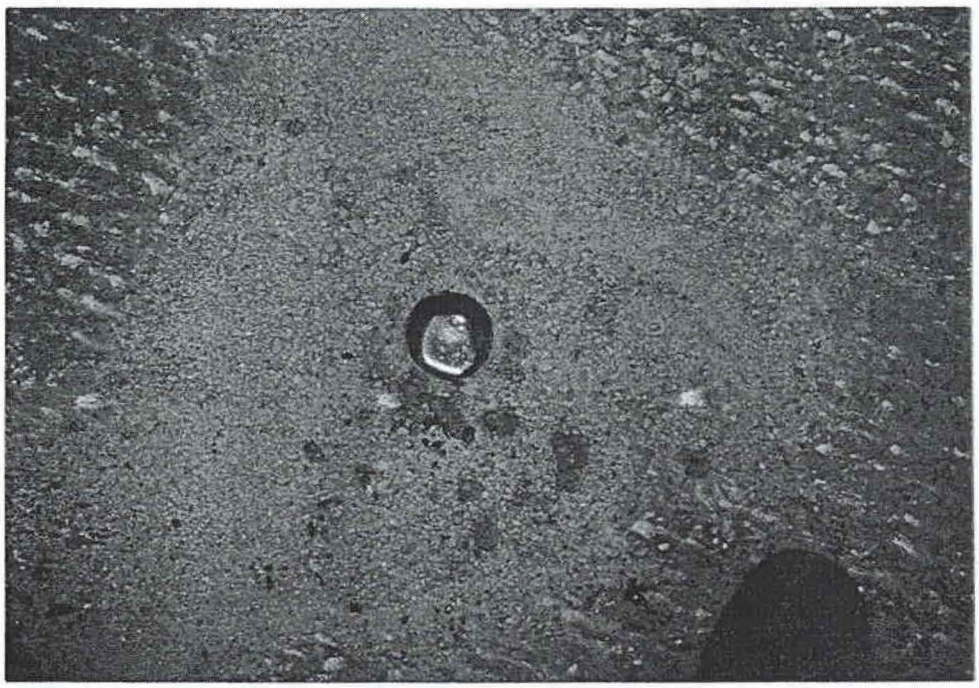

Water in Bottom of core hole.

Figure 39. IH 45 Houston - Ground Truth Evaluation, Water Found at Bottom of Test Hole.

Case 4. Base Evaluation-SH 158 District 6

Background

In 1988 State Highway 158 near Midland, Texas was reconstructed and widened to 4 lanes. The structure consists of a gravel sandy subgrade, 10 inches of crushed limestone and a 1.75 inch hot mix surfacing. Problems occurred during construction. Several sections of the asphalt ravelled extensively and had to be replaced. Major cracking was also observed shortly after the highway was opened to traffic in early 1989. This cracking was initially "block" in nature; blocks from 12" x 12" to 24" x 24" were common. This cracking progressed so that wide alligator cracks were evident along the entire job, see Figure 40. Several sections had to be patched. No other major distresses were present, no rutting was found. The highway carries a substantial number of heavy oil field trucks.

The district was considering a major rehabilitation to correct the problem. However, there were conflicting opinions as to the cause of the problem and the required treatment. One possibility was that the base had become saturated leading to rapid structural deterioration. Another was that the base was adequate and that the surface was the only problem.

A structural evaluation was conducted in March 1991 involving Falling Weight Deflectometer, Dynamic Cone Penetrometer and Ground Penetrating Radar survey.

GPR Survey Data Collection

The purpose of the GPR work was to evaluate the quality of the base course and to detect if localized "wet spots" were present. GPR surveys were conducted in both directions at 20 mph with a GPR trace being collected every 10 feet. After the complete site had been surveyed, a single test location was chosen to obtain ground truth base moisture content. At that location a single stationary GPR waveform was taken. A jack hammer was then used to remove the thin surfacing and samples of the base course were taken and returned to the laboratory for moisture content determination.

GPR Interpretation

A typical GPR waveform is shown in Figure 41. There are several items to note about this figure. First, because of the thin surfacing there is

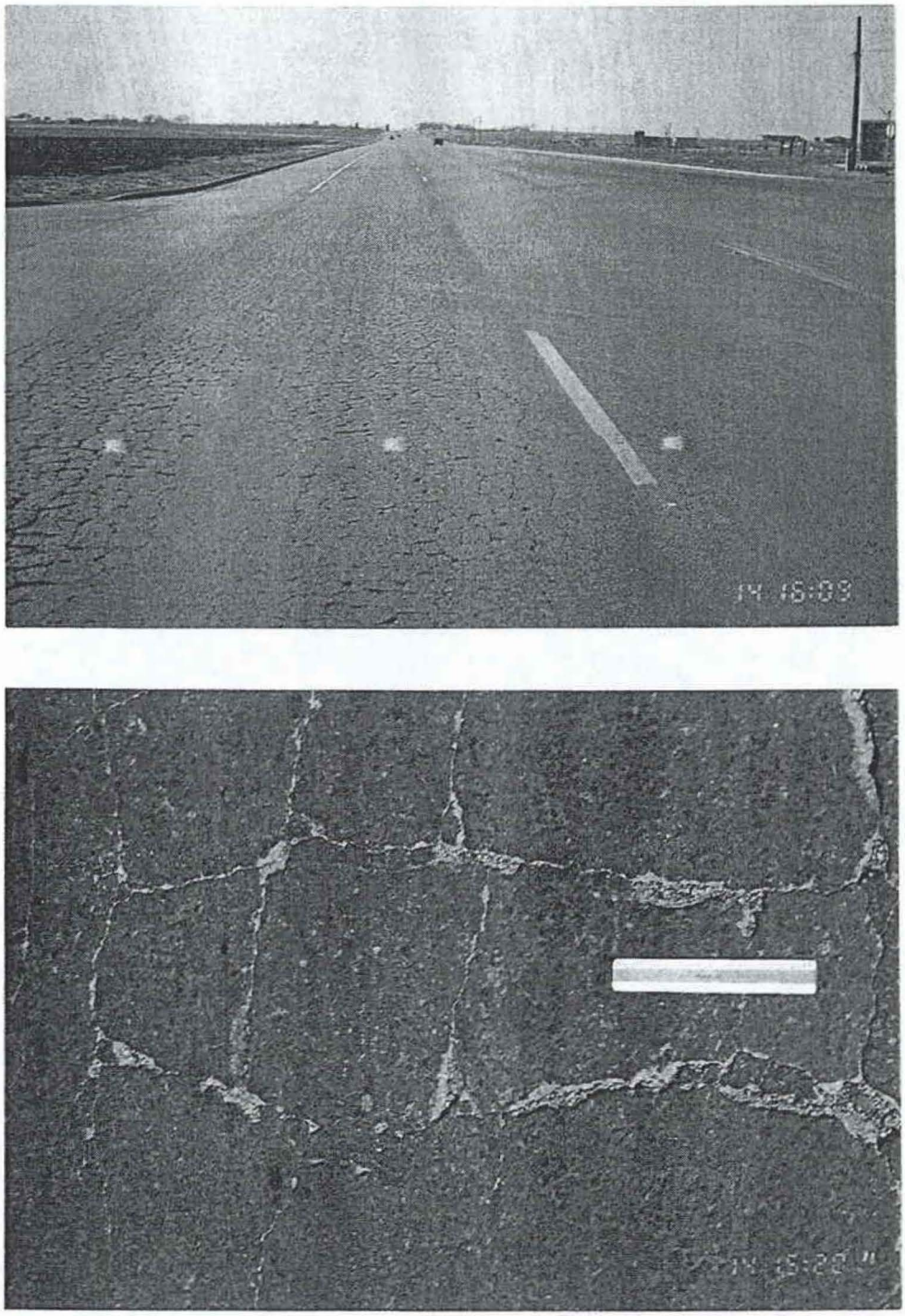

Figure 40. Surface Distress SH 158 - Midland, Texas.

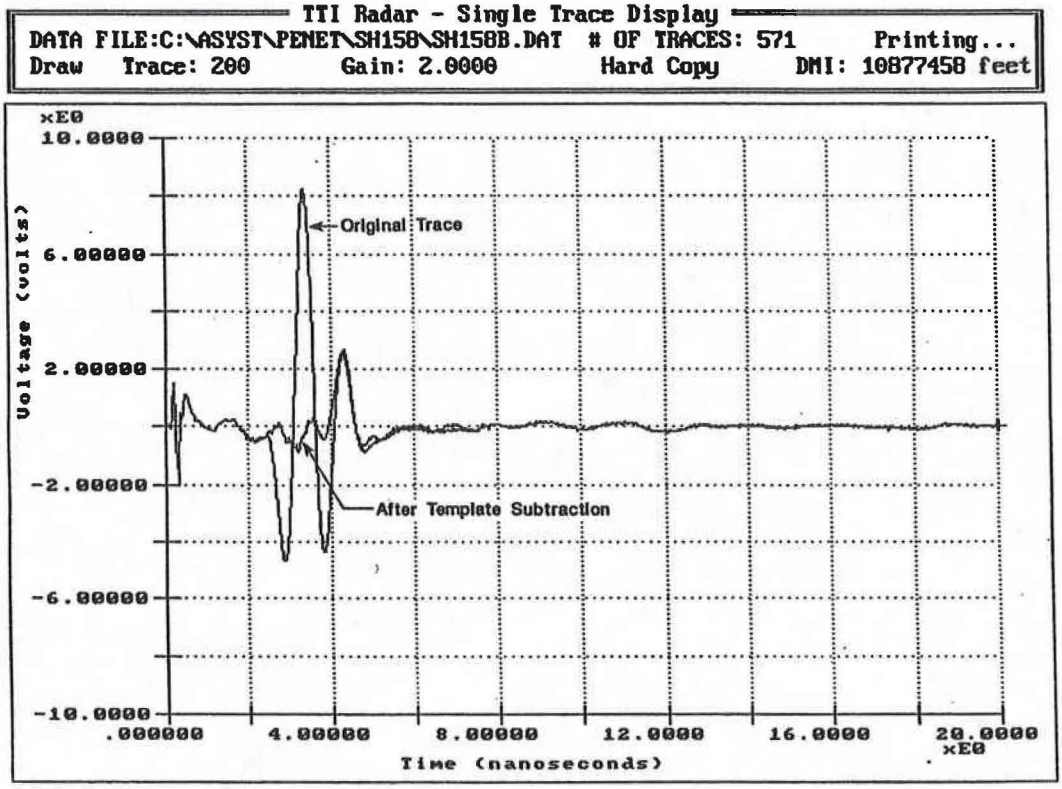

Figure 41. GPR Traces from SH 158 near Midland, Texas.

an overlap between the reflections from the top of the surfacing and the top of the base. Secondly, there is no reflection from the top of the subgrade indicating that there is no dielectric contrast between the base and subgrade. This is not surprising as the subgrade is a highly permeable sandy/gravel. In this instance it is impossible to use GPR to make base thickness measurements.

To evaluate the moisture content of the base course, it is necessary to use Equations 3 and 4 presented in Section 1 of this report. In order to obtain a reasonable amplitude of base reflection, a surface subtraction (template) was performed. The resulting waveform is also shown in Figure 41. The amplitude of base reflection was than used to calculate the dielectric of the base course. The results from the laboratory moisture tests were used to calibrate equation 4 to obtain an estimate for the unknown density ratio parameter. This density parameter was used to process all of the GPR waveforms for the entire roadway, resulting in the base moisture profile shown in Figure 42. In reviewing Figure 42 one other factor should be considered, it had rained about 0.25 inches the day before the GPR survey was conducted. The surface itself, as shown in Figure 40, is severely cracked. Bearing this in mind the variation in moisture content looked reasonable. The majority of the base course was calculated to have between 6 and 8% moisture, which is typical for crushed limestone base material. No areas of excessively high moisture content were found.

Conclusion

From GPR testing, it appeared that a wet base was not the problem with this highway. This was supported by both the Falling Weight Deflectometer and Cone Penetrometer test results, which concluded that the existing base was Class I material. Laboratory tests conducted on the asphalt extracted from the surfacing found that viscosity of the binder was very high, approximately twice as high as it should have been (from Thin Film Oven specifications). It was concluded that the asphalt was "burnt" during the construction process, resulting in a brittle mix which readily cracked. These results were accepted by the District staff, and the appropriate milling and resurfacing was undertaken.

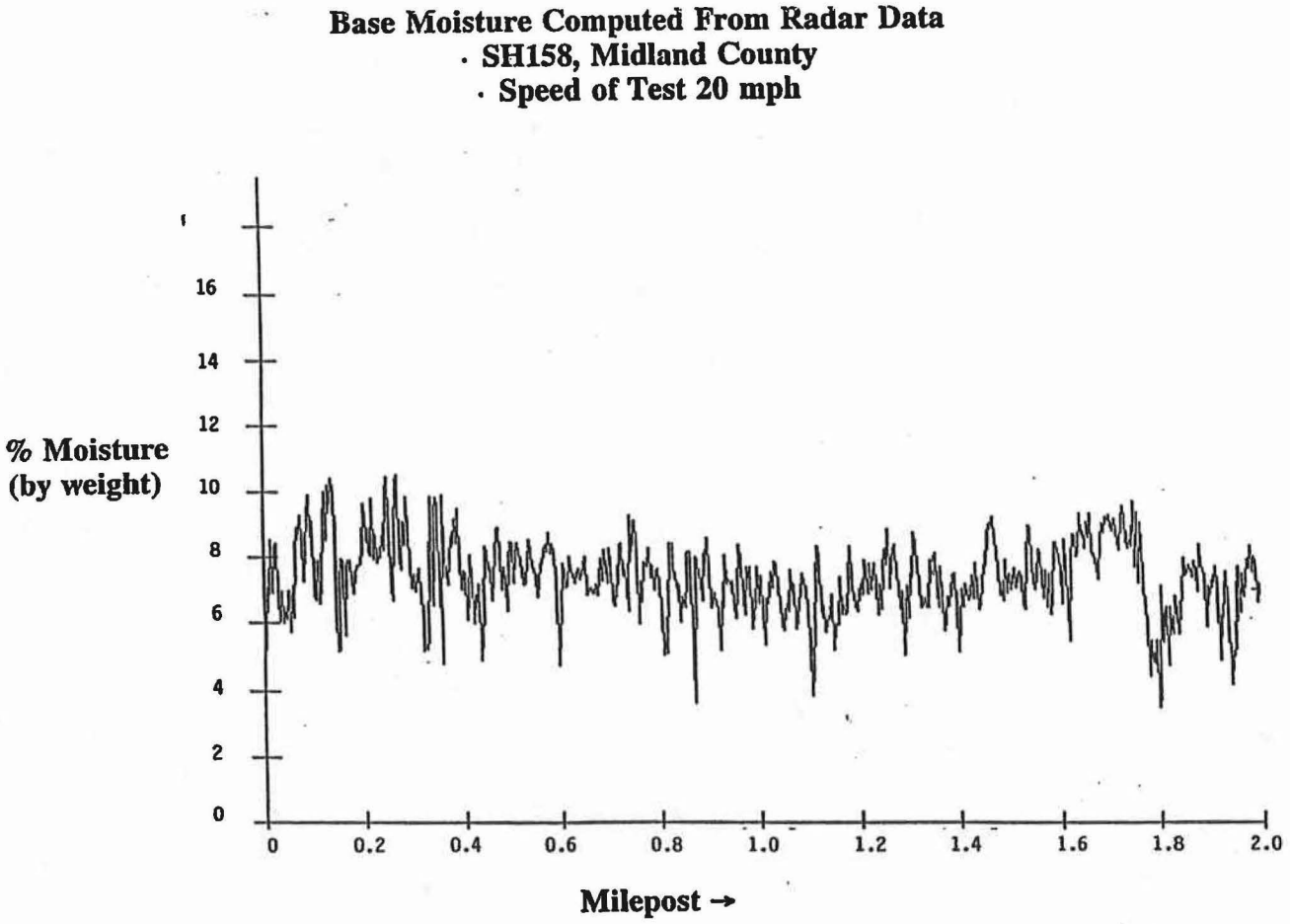

Figure 42. GPR Predicted Base Moisture Content for SH 158.

Case 5. Detection of Asphalt Stripping-US 96 District 11

Background

Up until 10 years ago a considerable number of hot mix asphalts were constructed with rounded river gravels as the coarse aggregate. These mixes were largely placed in the 1960's and 70's in east Texas where high quality crushed aggregates are not available. Many of these old mixes are prone to stripping and most have been buried with one or more asphalt overlays. Current TxDOT specifications, with minimum number of crushed faces and the use of antistripping agents, have tended to lessen the stripping problem. However, the existence of buried stripped layers is a major concern to engineers planning pavement rehabilitations. Stripping is a moisture related mechanism by which the bond between the asphalt and aggregate is broken, leaving an unstable low density layer in the asphalt. This low density area may or may not have moisture in it.

If possible, stripped layers should be detected and removed prior to placing the new overlay. The major issue becomes, Is stripping present? and how wide spread is it?. Small amounts of stripping can be removed by patching, large amounts will require extensive milling.

US 96 in District 11 is known to contain a stripped layer of asphalt. The total asphalt thickness is between 4.0 and 5.0 inches. The top two to three inches is relatively new overlays, generally in good condition, although substantial cracking is observed to be reflecting from below. The bottom two inches of the hot mix, being the original surface, is extremely variable. The section under consideration for rehabilitation is 1 mile long. Coring at eight locations found substantial stripping of the lower layers in five of the eight cores. In two locations the lower layer had completely deteriorated into "pea gravel". Rehabilitation studies had already concluded that the entire surfacing needs to be replaced. However, the presence of such extensive subsurface problems was an opportunity to evaluate if Ground Penetrating Radar could be used to successfully locate this stripping.

GPR Survey and Results

A GPR survey was conducted with a waveform collected at 5 foot intervals. Two waveforms from this section are shown in Figure 43 and Figure 44. Figure 43 was taken from a location where the asphalt layer was

found to be "sound" from the coring. In Figure 43a the surface peak and reflection from the top of the base are clearly visible. Figure 43b shows the effect of template subtraction (to remove the surface reflection from Figure 43a). Between 6 and 8 nanoseconds the small peak indicates a different asphalt layer, whereas the second layer peak indicates the top of the base. The second asphalt layer will have a slightly higher dielectric than the surfacing; this is a common occurrence.

Figure 44 shows a GPR waveform taken in an area of substantial stripping. Figure 44a shows the raw trace. Multiple peaks are present in the asphalt and the surface echo is distorted just after 6 nanoseconds. The results of the template subtraction are shown in Figure 44b. This time a substantial negative peak is observed just after 6 nanoseconds, indicating a low dielectric layer. A lower dielectric layer is indicative of a low density layer in the asphalt. Dielectric estimates using the TTI software computed the top layer of the asphalt to have a dielectric of 5.4 with the lower layer being 2.9. In this instance, the large negative peak appears to indicate substantial stripping.

Conclusion

GPR does appear to have some potential to detect stripping in asphalt layers, however, several issues need further investigation, namely:

1. The waveforms presented indicate that stripping is associated with a negative peak, indicating a dry low density layer. However, in some instances the stripped layer may have moisture in it; in that case the waveform may be substantially different.
2. The traces collected on US 96 were extremely variable. Approximately 20% were similar to Figure 43; another 20% were similar to Figure 44. The remaining 60% were somewhere between the two, with multiple minor peaks occurring between 6 and 8 nanoseconds. Currently there are no criteria for interpreting these traces. Further work needs to be done in defining levels of deterioration and relating them to GPR waveforms.

The District is interested in defining what percentage of the pavement has severe stripping. On this job, the highway sections could be broken up into severely stripped and unstripped (sound) sections. The majority of the section lies somewhere between the two with presumably some level of asphalt degradation. More work is needed in using GPR to detect stripping. The technology does, however, appear to have potential.

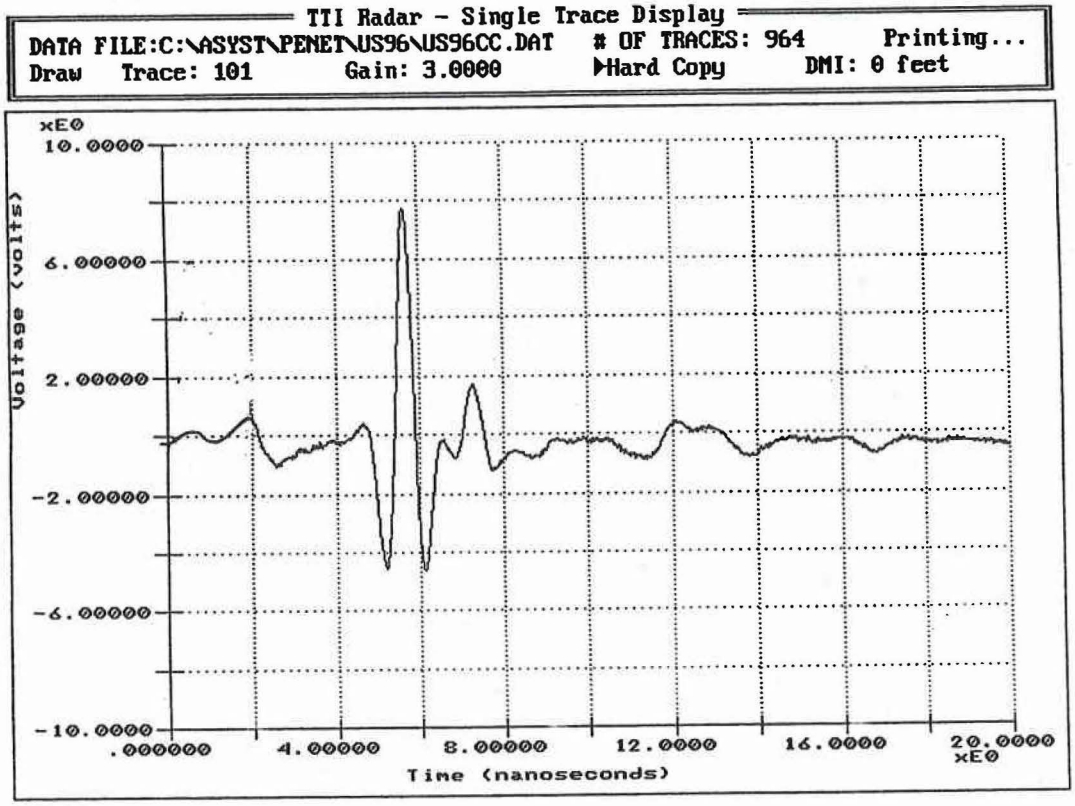

a. Original Trace

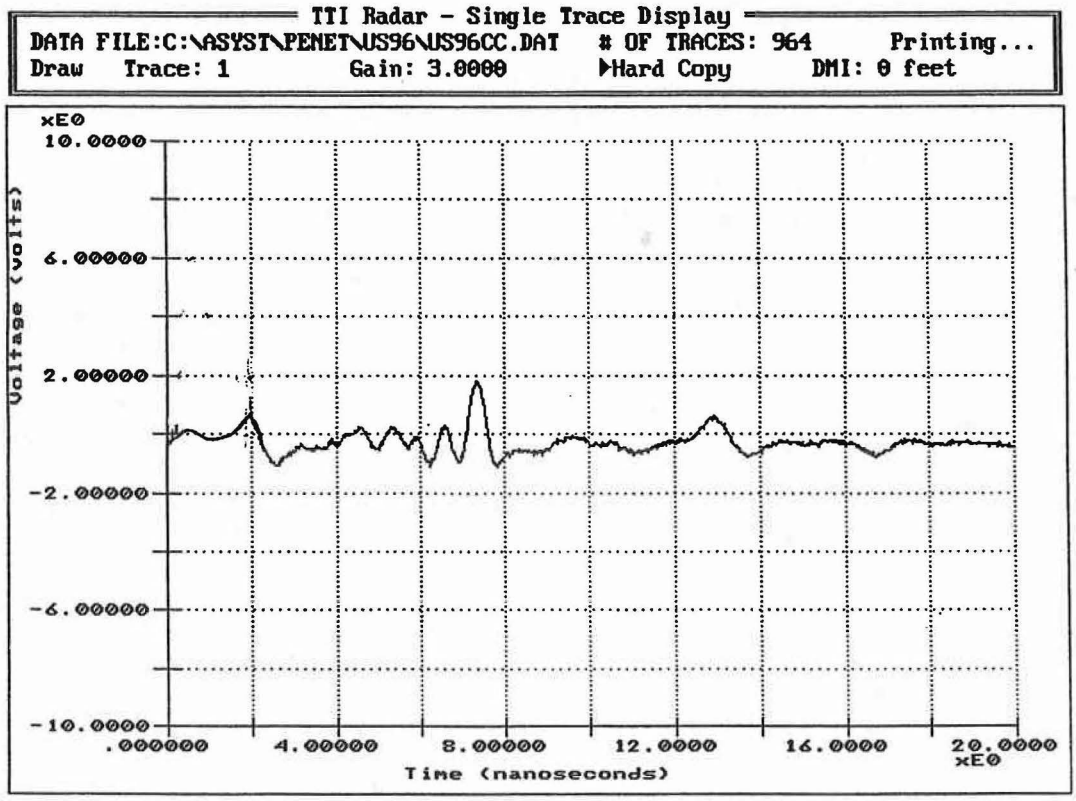

b. After Template Subtraction (Surface Reflection Removal).

Figure 43. GPR Waveforms from a Non-stripping Location on US 96.

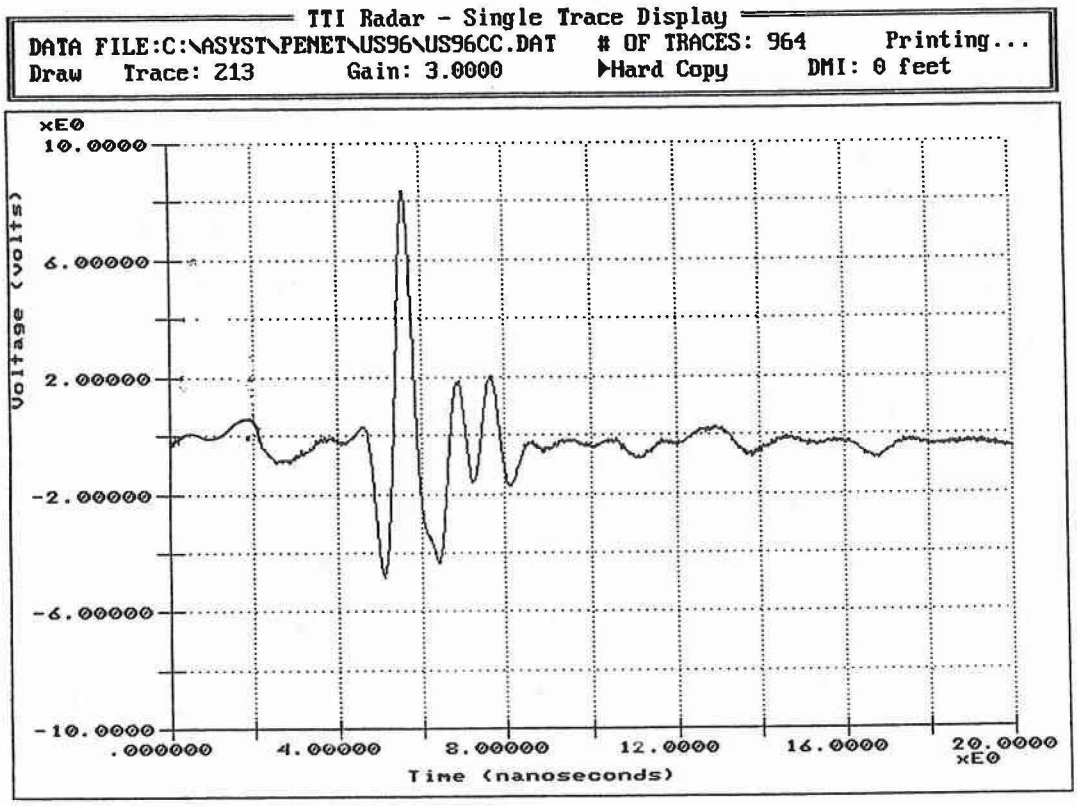

a. Original Wave Form.

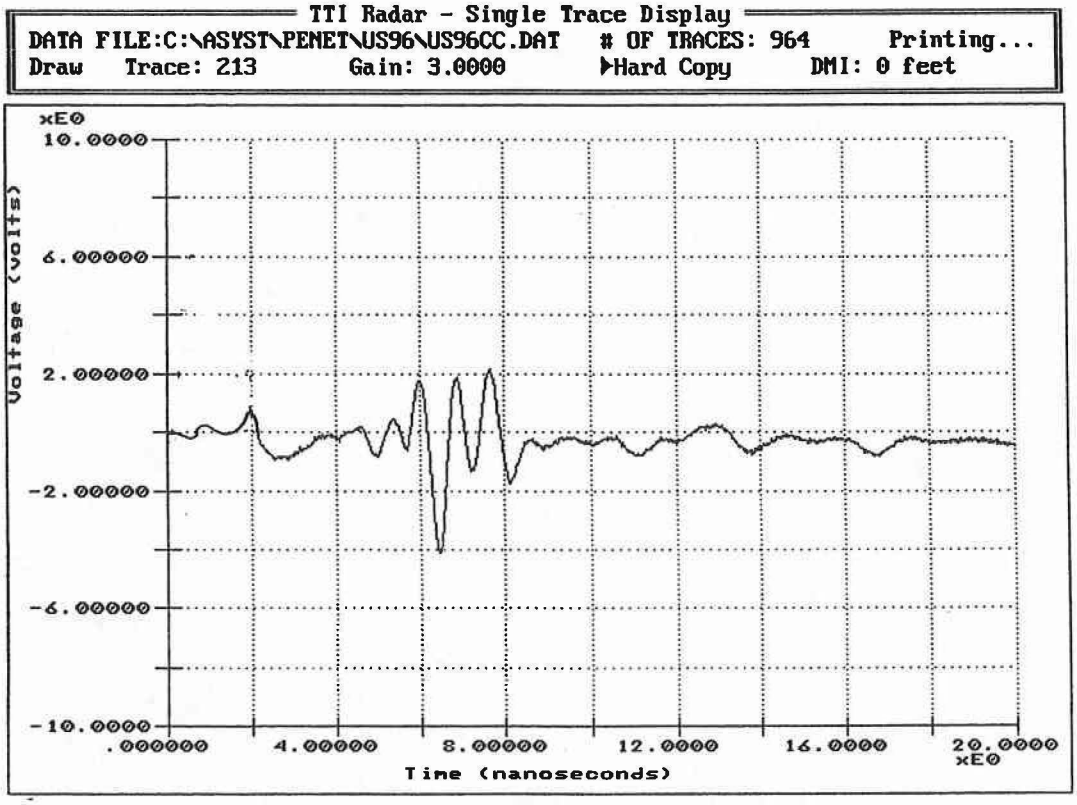

b. After Template Subtraction.

Figure 44. GPR Waveforms from a Stripping Location on US 96.

5. CONCLUSIONS AND RECOMMENDATIONS

This report has described both the hardware and software developed and implemented in the course of Study 1233. The Penetradar PS-24 Unit has performed well for almost two years with minimum maintenance. The PS-24 generates a stable monocycle 1 nanosecond pulse with little clutter or jitter. The focus of the research effort has been to develop signal processing algorithms for processing the return waveforms. The signal processing approach described in this report holds great promise for future developments. GPR waveforms provide a wealth of information about subsurface pavement conditions and only a portion of it is being used in current processing routines. The challenge to researchers is to convert these signals into meaningful information in a timely manner for pavement engineers.

A summary of the current systems capabilities is presented below:

For asphalt layer thickness determination, the system appears capable of estimating thickness to within 5% for the asphalt layer without taking a core. Thicknesses of up to 24 inches have been accurately measured.

For base thickness determination, thicknesses can be estimated, providing that there is a dielectric (moisture) contrast between the base and subgrade. This is not always the case, particularly with granular bases over sandy subgrades.

For stripping detection, a limited amount of work has been done in this area. It appears that severely deteriorated areas can readily be detected. Also GPR can be used to detect "sound" areas. Work needs to be performed in determining the influences of slight to moderate stripping on GPR waveforms. Additional signal processing and pattern recognition algorithms need to be developed.

For concrete thickness determination, the accuracy is not yet defined. However, it will probably be less accurate than for asphalt layers. The following issues complicate the processing of waveforms from concrete pavements:

1. Concrete (PCC) attenuates GPR waves more than asphalt layers. The layer thickness calculations used in this report assume that the attenuation is zero.
2. In its early life the electric properties of concrete are changing rapidly as the cement hydrates. The best time to test concrete is yet to be determined.
3. Thick slabs may contain multiple layers of reinforcing steel which make signal interpretation more difficult.
4. Most of the bases used beneath PCC slabs are stabilized, primarily asphalt bond breakers. The dielectric contrast between the PCC and asphalt layer may be insufficient to give an adequate interface reflection.

The application of GPR to concrete layer thickness determination is the subject of current research efforts at the Texas Transportation Institute.

For void detection, GPR can detect the presence of high levels of moisture beneath PCC slabs. However, this does not mean that a void is present. The two case studies presented in section 4 highlight this. If the base material is cement stabilized the moisture will probably be related to a void. If the base material is unstabilized there may or may not be a void. In all cases validation cores need to be taken. The epoxy core test is recommended for validation. If a moisture filled void is present, it will be detected by GPR, independent of void thickness. However, in this case it will be impossible to estimate void thickness. For air filled voids, it is thought that the current system will not have sufficient penetration power to identify small voids of less than 1/2 inch thickness. Large air voids probably can be detected.

In general it is concluded that the current system works well. There are several areas were GPR technology can be used to assist TxDOT engineers in evaluating pavements. Areas of future development include:

a. The development of a new generation of GPR systems. The current hardware is at least 10 years old, and many advances have been made in microwave technology. One area could be the development of a more powerful unit to permit penetration of thick concrete structures. Another could be a higher frequency system to give more near surface precision, this could be used for quality control of asphalt overlays.

b. The development of a mobile, perhaps a hand held unit, for void demarcation. Field personnel need a simple to use unit to be able to define the areas requiring undersealing.

c. Laboratory and field testing of pavements containing various levels of stripping.

d. Models of Electromagnetic wave propagation in attenuating layered systems already exist. These models need to be applied to interpreting waveforms from concrete pavements.

e. Developing a more fundamental understanding of the individual component dielectrics of typical layer materials (asphalt, aggregates, etc.) and how these interrelate to produce the composite dielectric of the pavement layer.

REFERENCES

1. ASYST, ASYST Software Technologies, Rochester, New York 14623.
2. Chung, T. and Carter, C.R., "Pavement Thickness Determination and Detection of Pavement Cavities Using Radar," Report MAT-91-03, Research and Development Branch, Ontario Ministry of Transportation.
3. Maser, K. R. and Scullion, T., "Automated Detection of Pavement Layer Thicknesses and Subsurface Moisture using Ground Penetrating Radar," Transportation Research Board paper, January 1991.
4. Maser, K. R., Scullion, T. and Briggs, R., "Use of Radar Technology for Pavement Layer Evaluation," Texas Transportation Institute, Research Report 930-5F, February 1991.
5. Operations and Maintenance Manual, Model PS-24, Penetrator Corporation, Niagara Falls, New York, 1990.